

6. STRUCTURAL ANALYSIS

In the previous chapter all available data pertaining to the nature and geometry of tectonic structures in the Bushveld Complex and surrounding areas were presented. In this chapter, this data will be analyzed in order to obtain an indication of stress conditions during various stages of the evolution of this portion of the Kaapvaal Craton. Stress is a tensor, defined as force per unit area which acts on a body (Lapidus, 1990). Generally, the strain observed in the rock record today is the result of these ancient tectonically induced forces. Therefore, stress analysis are used in this study in order to unravel the ancient stress fields which were responsible for the deformation observed in the Bushveld Complex and surrounding areas.

The most useful tool in stress analysis of the Bushveld Complex area is the application of Anderson's (1951) theory of faulting and dyke formation. Anderson (1951) proposed that when a homogeneous rock mass, close to the Earth's surface, is subjected to a stress field, then structures will form in predictable orientations, and the type of structure that will form, depends on the relative orientations of the principal stresses (σ_1 , σ_2 , and σ_3). In this study σ_1 is regarded as the maximum compressive stress, σ_2 the intermediate compressive stress and σ_3 the minimum compressive stress or maximum extension direction.

The structural analysis of the Bushveld Complex and surrounding areas involved the graphical representation of the orientations of each type of structural feature (dykes, lineaments, faults and folds) as present in the BOSGIS data base. The data are presented as rose diagrams from which principal trends are determined statistically (see Chapter 2). This process ensures that possible errors in the strike of low-angle structures are reduced. Using these directions, principal stress directions can then be determined. Structural analyses were further constrained by the incorporation of published data. Stress direction for folds and faults are interpreted during the following geological time periods; pre-Transvaal, post-Transvaal/pre-Bushveld, post-Bushveld/pre-Waterberg, post-Waterberg/pre-Karoo, Pilanesberg (only Bos2 structures) and post-Karoo. The ideal would have been to analyse stress directions for dykes and lineament during the same geological time periods. However, ages for dykes and lineaments are mostly unknown, and therefore structural domains were chosen based on the preferred orientations as well as the rock types in which these

structures occur. Stress directions were then interpreted according to the various structural domains.

Dykes are generally considered to be vertical features which formed as a result of In order to determine stress conditions for the various structures at the various geological times periods, certain assumptions had to be made:

1. The intersection of any specific feature with the map surface is the true strike of the feature. This is always true for vertical structures such as dykes, but may give erroneous results for low-angle structures such as thrust faults, or axial planes of folds, especially in areas of high relief.
2. Rocks are homogeneous and no pre-existing weaknesses are present (cf. Anderson, 1951). This is rarely the case, and many structures are known to have reactivated along pre-existing weaknesses. Therefore, even though a stress is not applied in the optimum orientation according to Anderson's (1951) theory, a pre-existing weakness might reactivate in response to an oblique stress direction. In this study, stress directions for structures which are known to have reactivated, are interpreted to have formed under the proposed stresses of Anderson's (1951) theory for homogenous rocks.

A geological map of the Bushveld Complex area. In the second part of this chapter the strike and dip data of the BOSGIS data base are analyzed by means of stereographical plots. Generally, stereographical plots were made according to the ages of the rocks in which strike-and-dip values were measured, thereby defining structural domains. Density distribution analysis and principal direction analysis are the main methods by which these plots were analysed. The regional geometry of the various areas could be determined by means of this type of analysis. However, structural analysis was somewhat handicapped due to the irregular distribution of strike and dip values in the data base.

compositions obtained from the syenite dykes (B). The majority of the syenite dykes are more restricted to the eastern part of the Bushveld Complex, whereas dolerite dykes appear more frequently in the western part of the Bushveld Complex. Dolerite dykes are interpreted to have formed during the same time as the syenite dykes are related to the intrusion of the Bushveld Complex (see also 1990).

Both types of dykes are orientated mainly in the E-W direction (Figure 6.2). However, closer evaluation indicates that the dolerite dykes have a preferred orientation of 300° whereas the syenite dykes are orientated in the E-W direction. The following principal stress directions are indicated in Figure 6.3.

6.1 Stress analysis from Dykes

Dykes are generally considered to be vertical features which formed as a result of horizontal extension. Anderson's (1951) theory of dyke formation is illustrated in Figure 6.1. In this case σ_3 is perpendicular to the strike of the dyke, i.e. horizontal, while the dyke itself lies in the σ_1 - σ_2 plane. Thus, either σ_1 or σ_2 can be vertical.

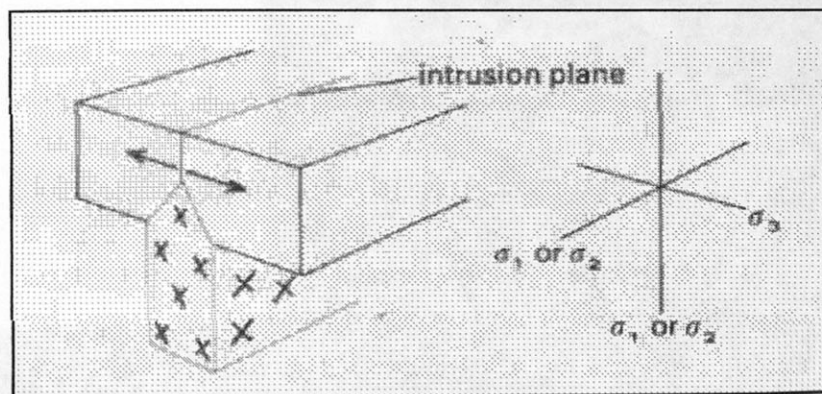


Figure 6.1. The emplacement of a dyke and the predictable stress directions according to Anderson (1951) (after Park, 1997).

A geological map of the Bushveld Complex and surrounding areas with all the dykes included in the BOSGIS database is shown in Figure 6.2. Dyke orientations for each structural domains of the respective Bos areas were analysed separately. Due to uncertainty of σ_1 and σ_2 directions, only σ_3 directions are mentioned in the text and indicated on the rose diagrams.

6.1.1 Bos2

Dykes occurring in the Bos2 area (Figure 6.3) were grouped based on their compositions obtained from the BOSGIS data base, namely dolerite dykes (A) and syenite dykes (B). The majority of the dykes are situated in granites, however syenitic dykes are more restricted to the granites of the Makoppa dome, whereas dolerite dykes appear more frequently in the granites of the Bushveld Complex. Dolerite dykes are interpreted to have intruded during post-Karoo times and syenite dykes are related to the intrusion of the Pilanesberg Complex (Keyser, 1997).

Both types of dykes are orientated more or less in the same direction (Figure 6.3). However, closer evaluation indicates that the dolerite dykes have a preferred orientation of 300° whereas the syenite dykes are orientated along a 320° direction. The following principal stress directions are therefore interpreted for the respective

Figure 6.2

Bosgis Dyke Map

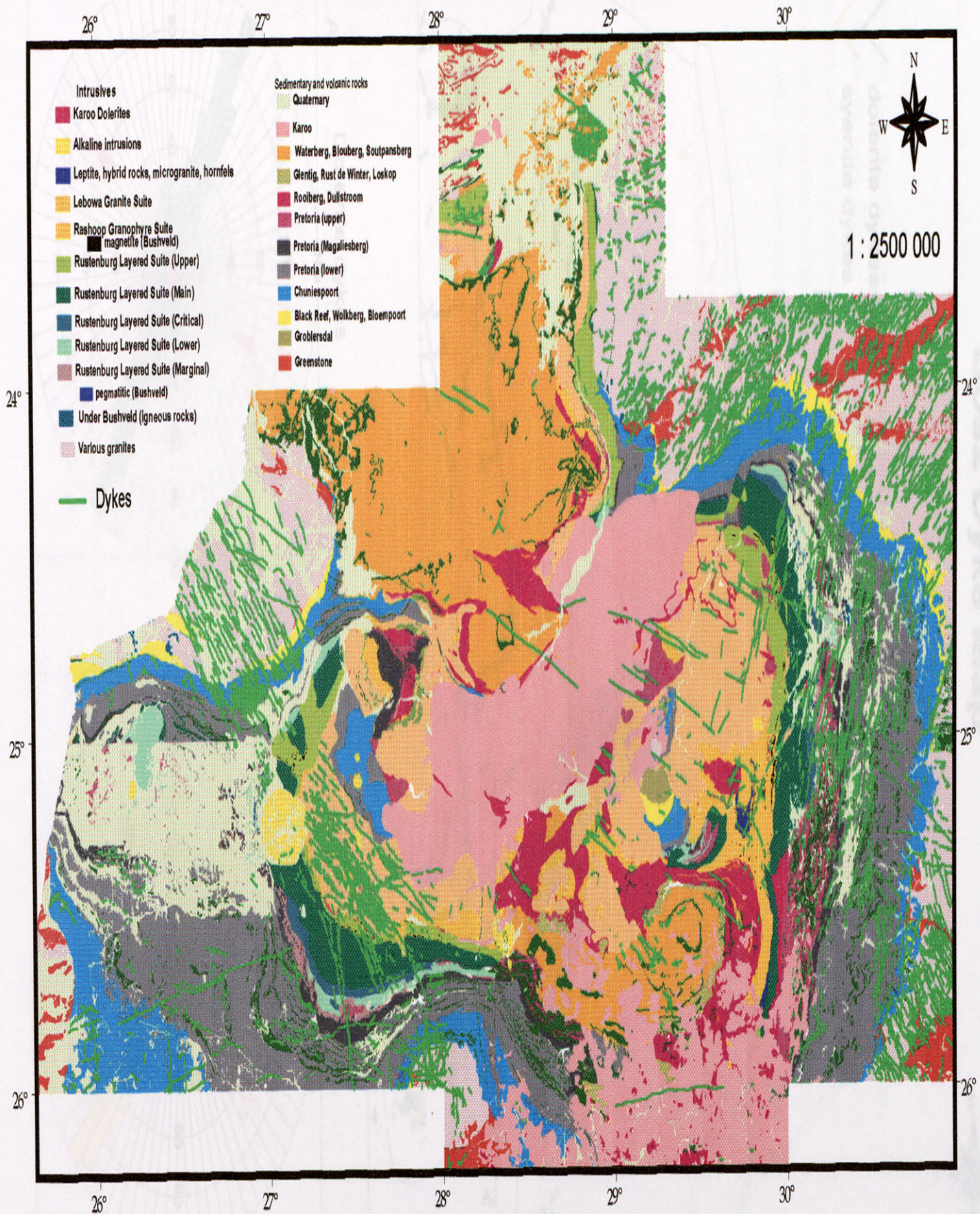
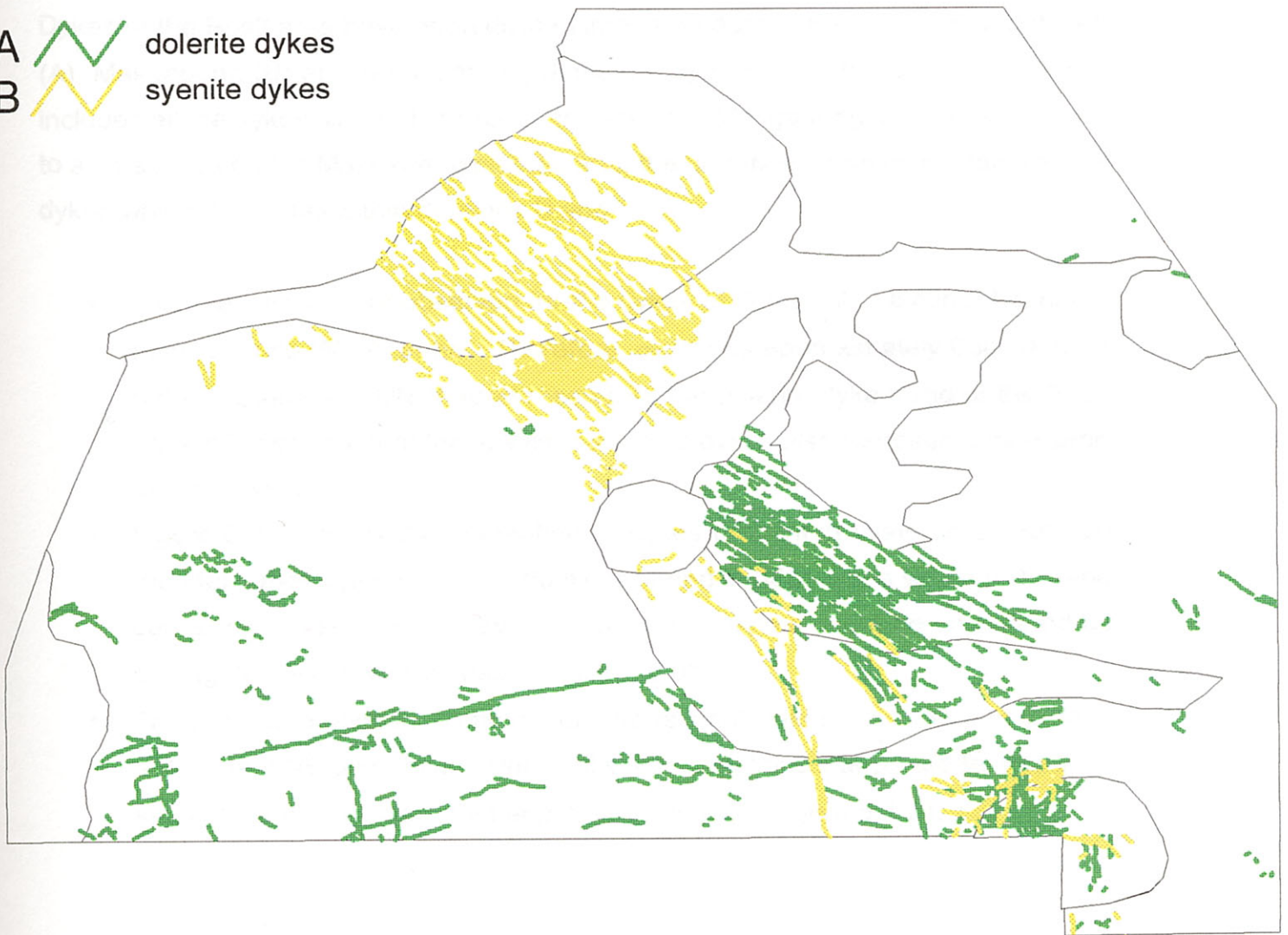


Figure 6.3

Bos2 Dyke Map

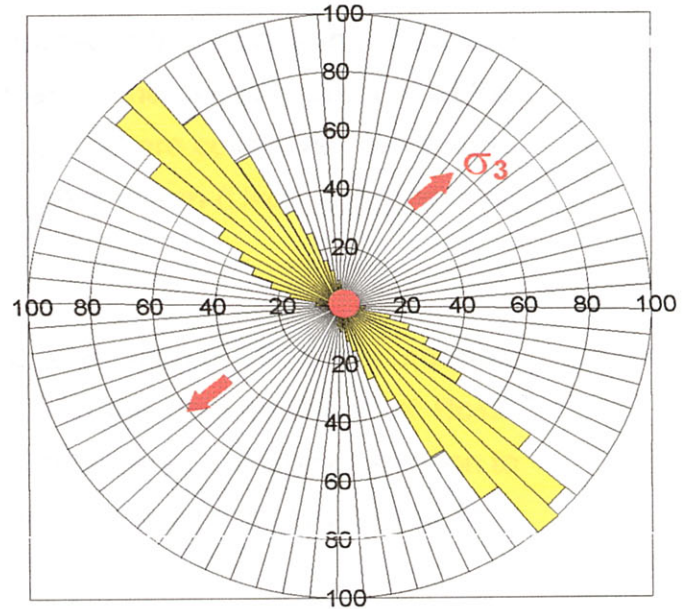
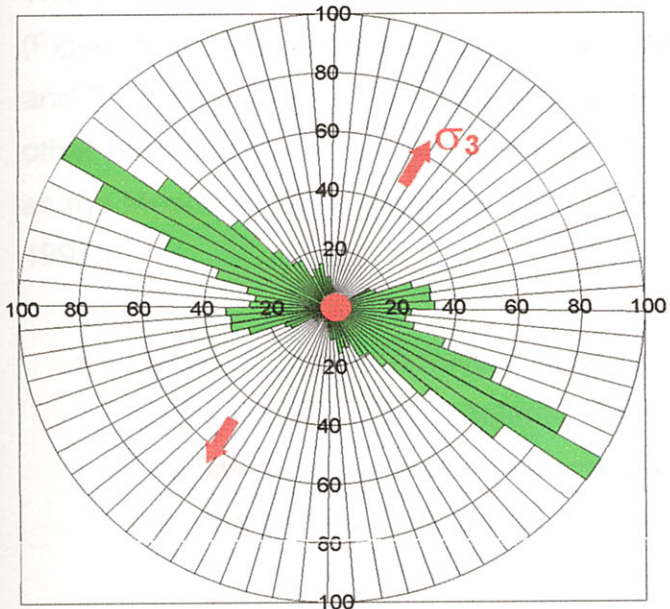


- A  dolerite dykes
- B  syenite dykes



A Dolerite dykes

B Syenite dykes



dyke sets: σ_3 trends 030° in the case of the dolerite dykes, and 050° for the syenite dykes (Figure 6.3 A and B).

6.1.2 Bos3

Dykes of the Bos3 area have been divided into three domains, namely an undefined, (A), Makgabeng (B) and Archaean (C) domain (Figure 6.4). The Archaean domain includes all the dykes situated in Archaean rocks, the Makgabeng domain is confined to a small area on the Makgabeng plateau and, the undefined domain contains all the dykes which do not fall within domains B and C.

- Two main trends are observed for the dykes of domain A, a minor NE and a more definite WNW trend. Therefore, σ_3 trends approximately 030° (Figure 6.4 A). Since the WNW trend resembles the dolerite dyke trend of the Bos2 area, it is possible that these WNW trending dykes also represent post-Karoo dolerite dykes.
- Figure 6.4 B shows the orientation of dykes present in Waterberg strata on the Makgabeng plateau. The dominant trend is 080° and a weak 100° trend can also be seen. These two orientations of dykes might be interpreted as conjugate sets, in which case σ_3 will trend 0° .
- The Archaean domain (C) hosts numerous small dykes which appear to have a dominant NE orientation. Principal stress directions interpreted for this dyke set, indicates a σ_3 orientated approximately 330° (Figure 6.4 C).

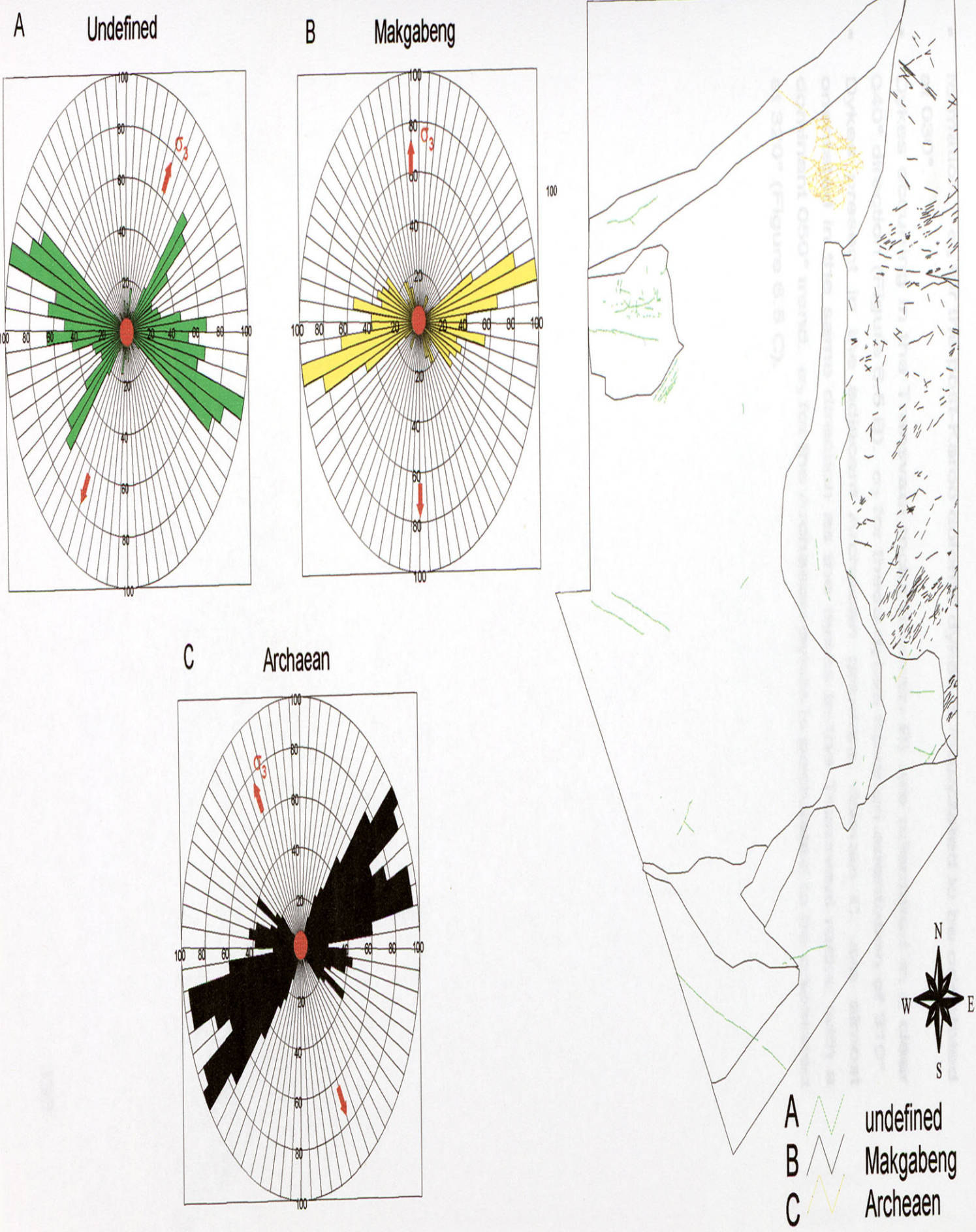
6.1.3 Bos5

The dykes occurring in the eastern Bushveld Complex area occur in three domains (Figure 6.5). The domains include all the dykes situated in the Archaean (domain C) and Transvaal (domain B) rocks respectively, as well as the dykes present in all the other formations (domain A). Dykes of domains B and C are collectively referred to as the Mesozoic Dyke swarm or the Olifants River dyke swarm (Uken and Watkeys, 1997a).

- Dykes of domain A have a strong preferred orientation of 290° , and probably represent post-Karoo dolerite dykes, similar to the dolerite dykes of Bos2. The few dykes orientated between 040° and 050° have a similar orientation to the Wonderkop fault trend, and are therefore possibly related to the fault

Figure 6.4

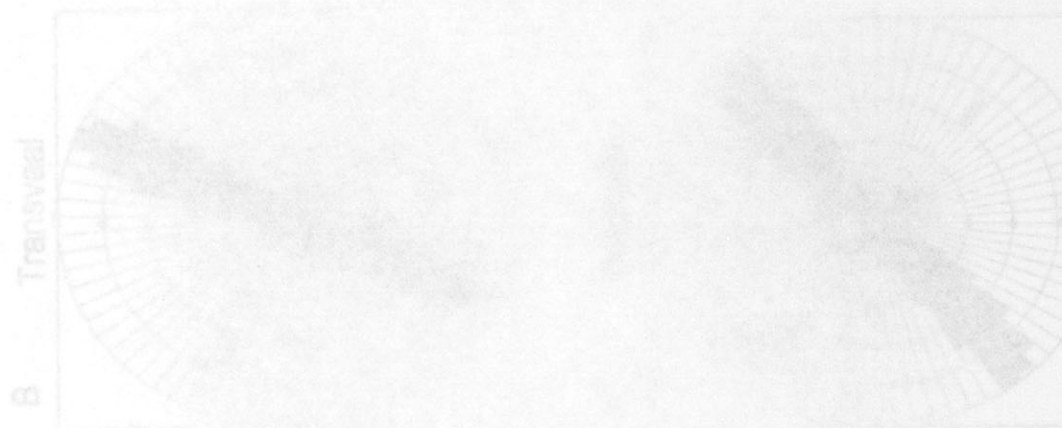
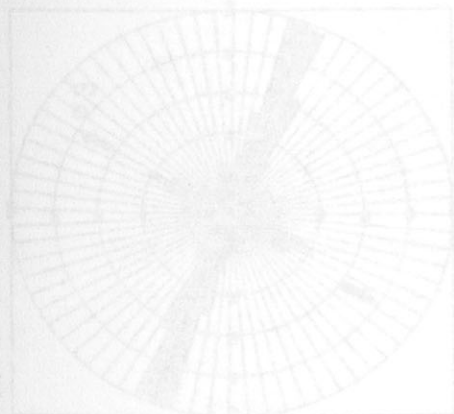
Bos3 Dyke Map



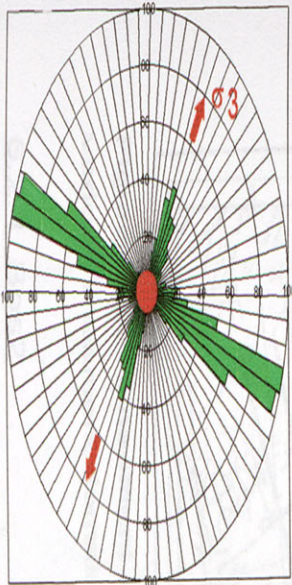
- formation. σ_3 for the post-Karoo dolerite dykes is interpreted to be orientated at 030°.
- Dykes occurring in the Transvaal rocks (domain B) are orientated in a clear 040° direction (Figure 6.5 B). σ_3 for these dykes have an orientation of 310°.
- Dykes present in the adjacent Archaean granites, domain C, are almost orientated in the same direction as the dykes in the Transvaal rocks, with a dominant 050° trend. σ_3 for the Archaean dykes is postulated to be orientated at 320° (Figure 6.5 C).

Bos5 Dyke Map

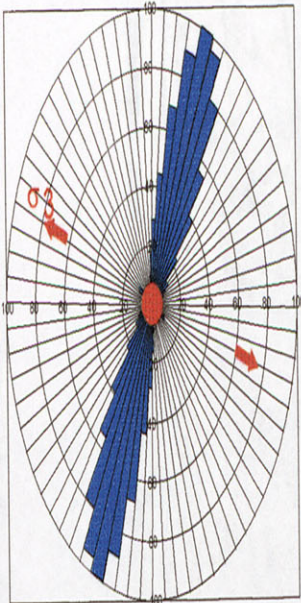
Figure 6.5



A Undefined



B Transvaal



C Archaean

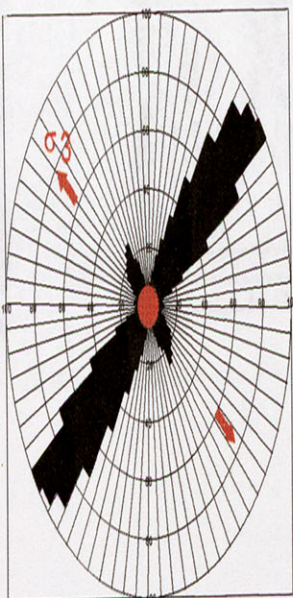


Figure 6.5

Bos5 Dyke Map



- A undefined
- B Transvaal domain
- C Archaean domain

6.2 Stress analysis from Lineaments

A lineament can be defined as a linear feature prominent enough to be recognized by regional observation techniques such as aerial photos, LANDSAT images, aeromagnetics, etc. In many cases it is unknown what these linear features represent, but in this study the assumption is made that lineaments reflect vertical joints, fractures, or dykes. Therefore, the interpretation of stress directions responsible for lineaments will be the same as for dykes.

Figure 6.6 shows a geological map with the locations of different types of lineaments in the Bushveld Complex area. The lineaments of each Bos area were considered separately according to the various structural domains. Sharpe and Lee (1990) presented a lineament domain map, defining six lineament domains (Figure 6.7), which are broadly similar to domains chosen for this study.

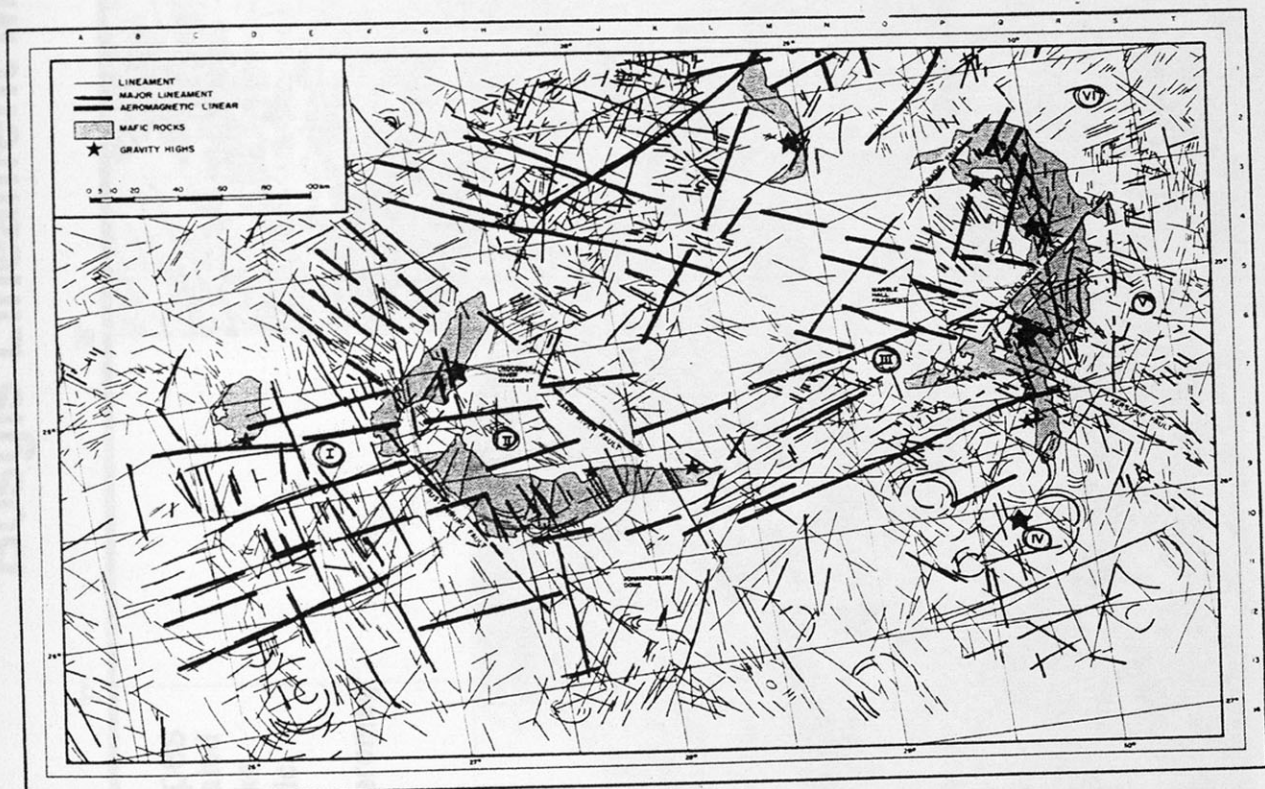


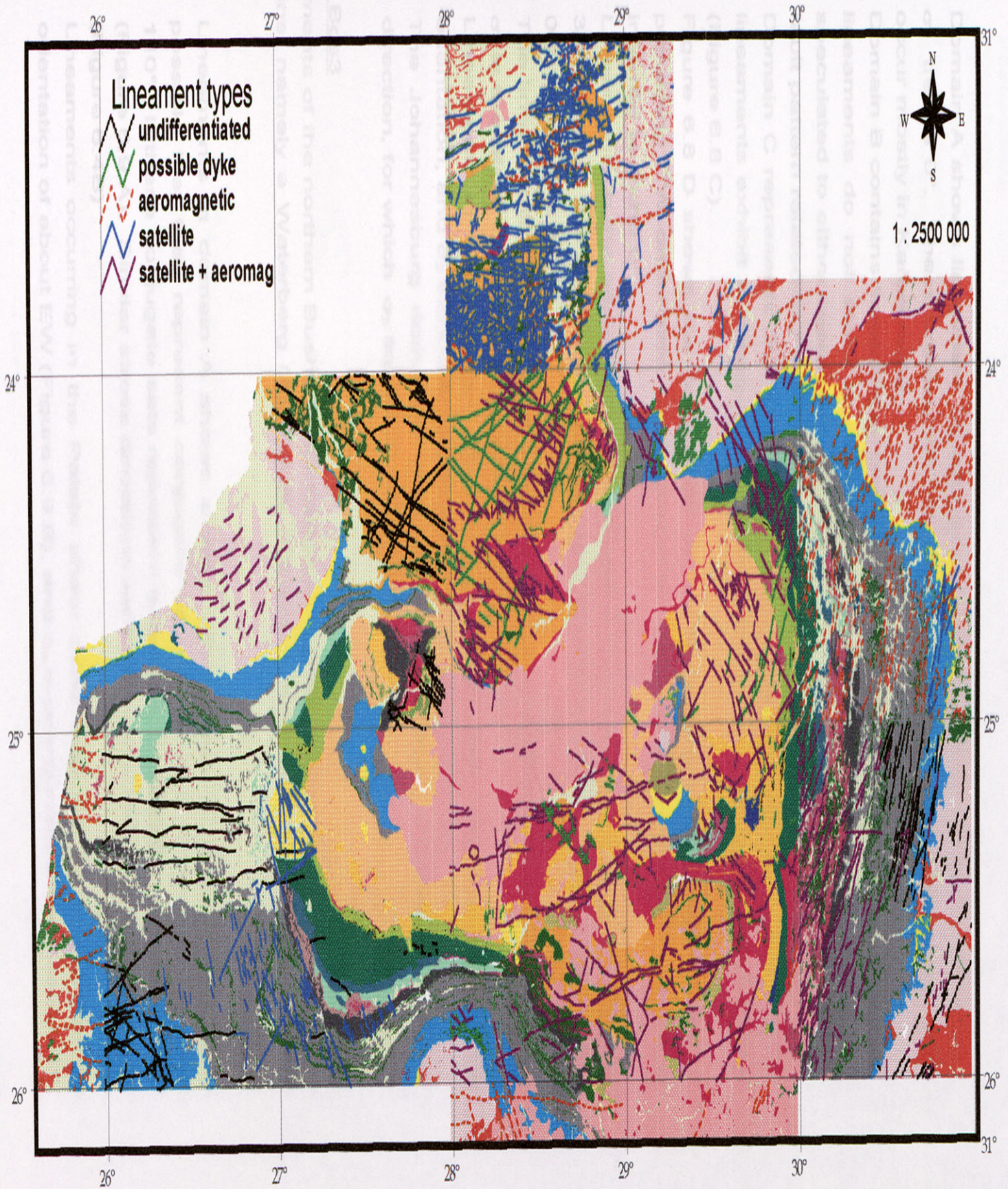
Figure 6.7. Lineament map of Sharpe and Lee (1990) with roman numbers indicating the various lineament domains.

6.2.1 Bos2

Figure 6.8 shows the eight lineament domains of the Bos2 area, they include a Karoo (A), Pilanesberg (B), Waterberg (C), far western Province (D), western

Figure 6.6

Bosgis Lineament Map



- Domain A shows lineament orientated about 90° (Figure 6.8 A). Therefore, σ_3 trends 0°. These lineaments are probably post-Karoo in age since they occur mostly in Karoo rocks.
- Domain B contains lineaments occurring in the Pilanesberg Complex. These lineaments do not show a preferred orientation and their significance is speculated to either represent conjugate joint sets, veins or might be a radial fault pattern related to the Pilanesberg Complex (Figure 6.8 B).
- Domain C represents lineaments occurring in the Waterberg rocks. These lineaments exhibit a strong trend of 290° and a σ_3 trending 020° is deduced (Figure 6.8 C).
- Figure 6.8 D shows the lineaments of the far western Transvaal basin. A prevailing EW orientation of aeromagnetic lineaments is present and σ_3 is inferred to trend 0°.
- Lineaments in the adjacent domain (E) have two main orientations of EW and 330° (Figure 6.8 E). σ_3 directions would therefore trend 0° and more or less 060° (Figure 6.8 E).
- The lineaments of the Rooiberg domain (F) have a general trend of 300° and σ_3 is therefore directed towards 030° (Figure 6.8 F).
- Lineaments in the Makoppa dome (G) are short and have a general ENE orientation, and σ_3 trends approximately 330° (Figure 6.8 G).
- The Johannesburg dome (H) host longer lineaments orientated in a EW direction, for which σ_3 trends 0° (Figure 6.8 H).

6.2.2 Bos3

Lineaments of the northern Bushveld Complex area are grouped into three structural domains, namely a Waterberg (A), Palala (B) and a Archaean (C) domain (Figure 6.9).

- Lineaments in domain A shows a wide EW spread of orientations. It is possible that they represent conjugate sets orientated at roughly 60° and 110°. If these conjugate sets represent extensional features, σ_3 will trend 0° (Figure 6.9 A). Similar stress directions were obtained from Waterberg dykes (Figure 6.4B)
- Lineaments occurring in the Palala shear zone area (B) have a preferred orientation of about EW (Figure 6.9 B), and σ_3 is interpreted to be directed 0°.

Figure 6.8

Bos2 Lineament Map

University of Pretoria and Grewensteyn, R M (2001)

- A  Karoo
- B  Pilanesberg
- C  Waterberg
- D  Rooiberg
- E  Western Province
- F  Far western Province
- G  Johannesburg dome
- H  Makoppa dome

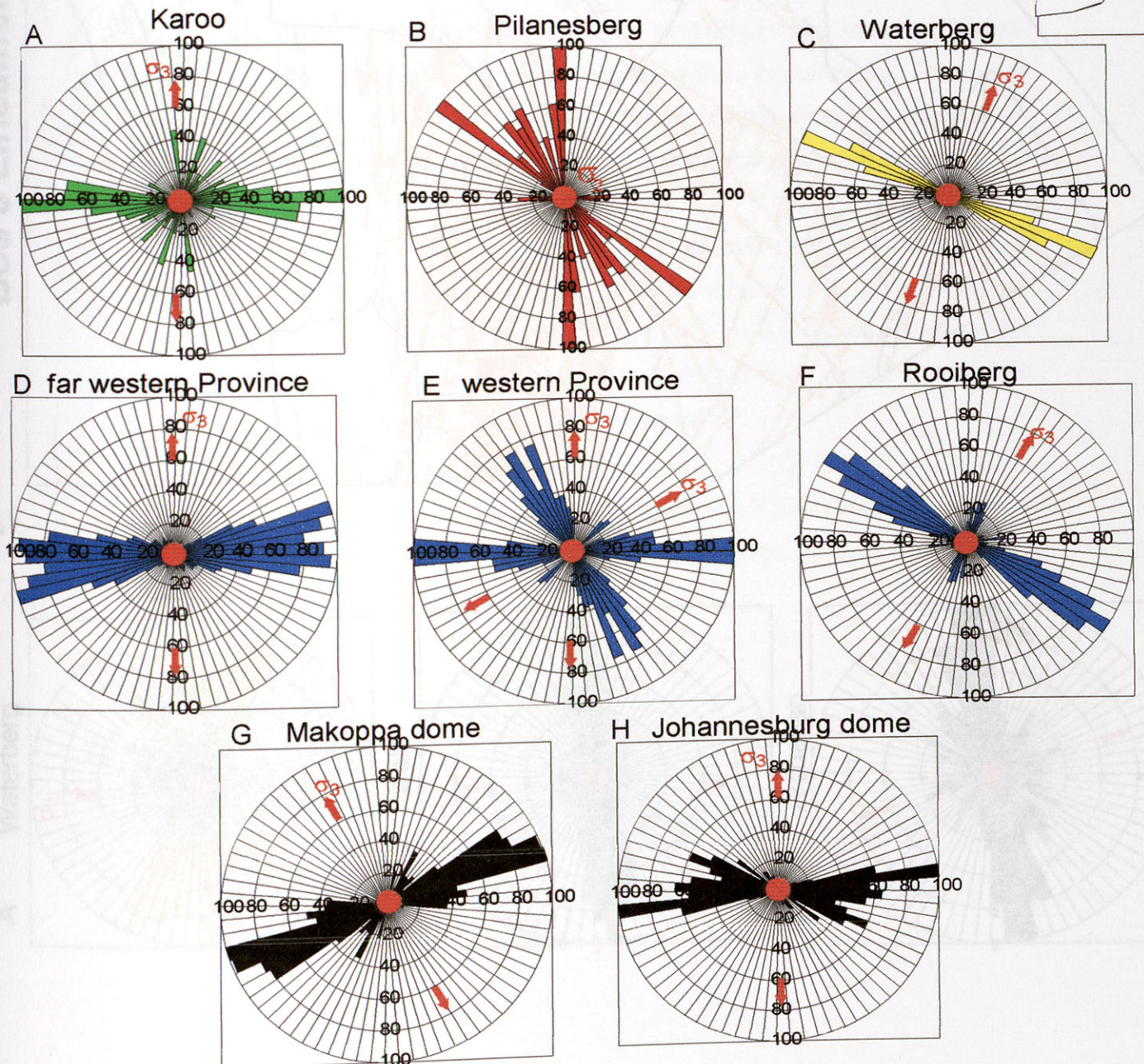
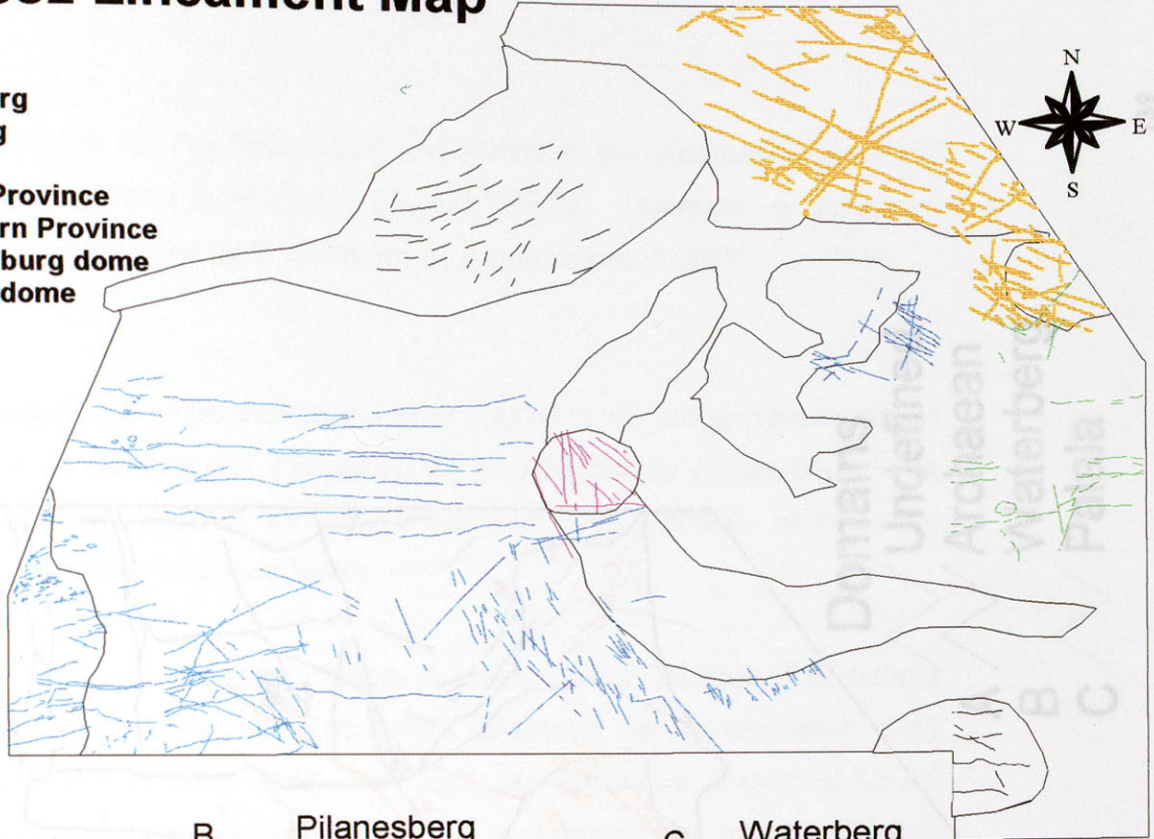
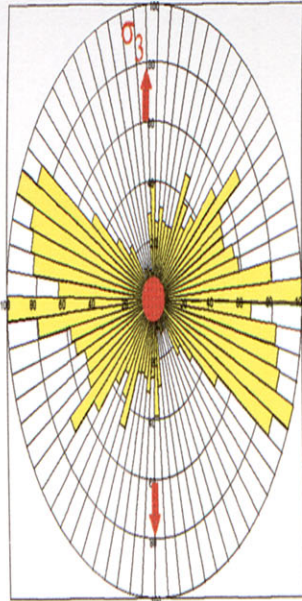


Figure 6.9

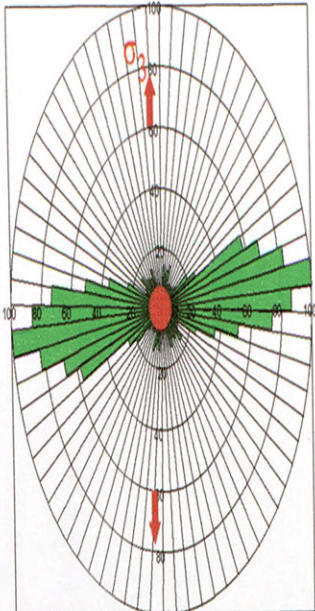
Bos 3 Lineament Map



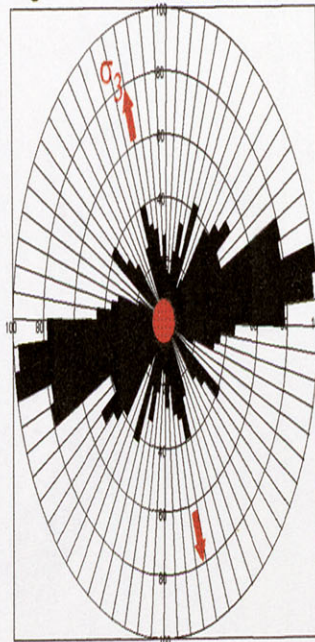
A Waterberg



B Palala



C Archaean



- Domains**
- Undefined
 - A Archaean
 - B Waterberg
 - C Palala

- The rose diagram for the lineaments positioned in the Archaean rocks (C) display fairly scattered orientations (Figure 6.9 C). However, a dominant 080° trend can be recognized, for which σ_3 is orientated at 350°.

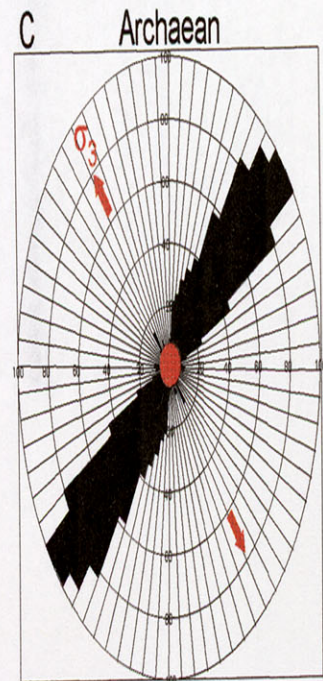
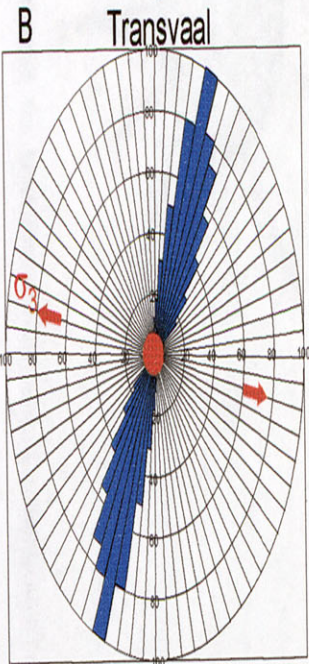
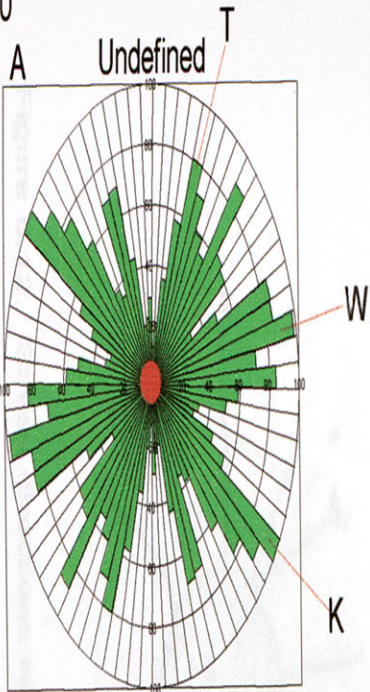
6.2.3 Bos5

Lineaments of the eastern Bushveld Complex area (Figure 6.10) are grouped in three domains namely, an Undefined (A), Transvaal (B) and Archaean (C) domain. The first domain is undefined since it contains lineaments with variable orientations occurring in different regions and rock types

- The rose diagram representing domain A shows a wide scatter of directions (Figure 6.10 A). However, three dominant directions can be deduced; they include the 030° (T), 080° (W) and 330° (K) directions (Figure 6.10 A). These three directions coincide with dyke and lineament trends of other Bushveld areas. The 030° trend resembles dykes occurring in Transvaal rocks of domain B, the 080° trend equals Waterberg age lineaments of Bos3, and the 330° trend coincides with the Karoo dolerite dyke direction throughout the Bushveld Complex area.
- Domain B hosts lineaments occurring in the Transvaal rocks and have a very strong 020° orientation (Figure 6.10 B). This direction corresponds with the orientations of the dykes in the same domain (Figure 6.5 B), and also similar to trend (T) above. It can therefore be deduced that these lineaments probably represent dykes for which σ_3 will trend 290°.
- The lineaments of domain C trend more or less in a 050° direction and σ_3 is interpreted to be directed towards 320° (Figure 6.10 C). These directions correspond to directions obtained for the Olifants River dyke swarm (Figure 6.5 C).

Figure 6.10

Bos 5 Lineament Map



- A Undefined
- B Transvaal domain
- C Archaean domain

6.3 Stress analysis from Faults

Many different types of faults occur in the Bushveld Complex and surrounding areas. Anderson's (1951) theory of faulting was used to derive stress directions for the faults in the study area (Figure 6.11).

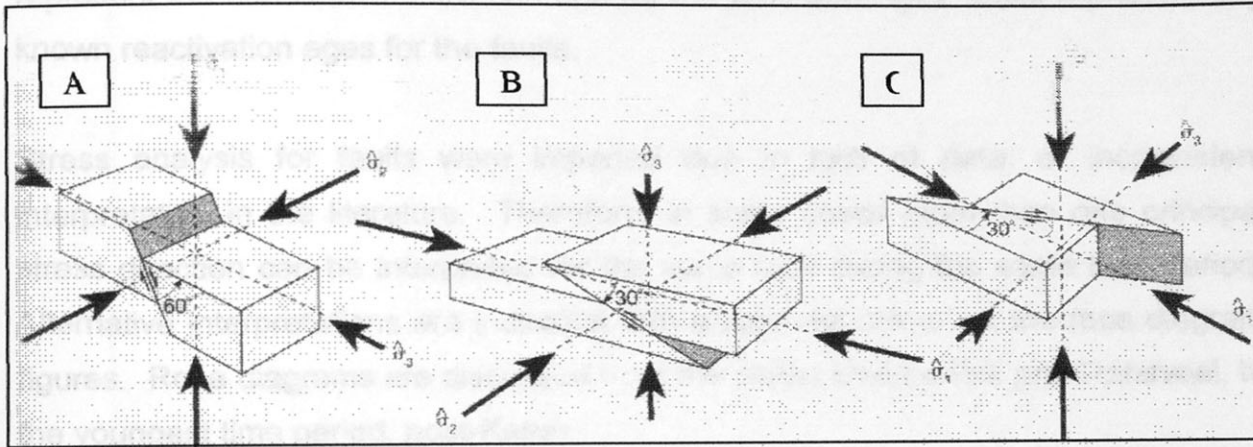


Figure 6.11. Anderson's (1951) theory of faulting, showing the relationship between the orientation of the principal stresses and the different ideal fault types. A. Normal fault with maximum compressive stress σ_1 vertical. B. Thrust fault with minimum compressive stress σ_3 vertical. C. Strike-slip fault with intermediate compressive stress σ_2 vertical (after Twiss and Moores, 1992).

Special consideration is necessary when analysing the stress directions for faults resulting from the intrusion of a magmatic dome, such as Pilanesberg. Generally faults will occur in a radial pattern around the intrusion (Figure 6.12). Principal stress direction, σ_1 and σ_2 might be vertical depending on the distance from the dome. Around the dome faults are the result of a vertical σ_2 and horizontal σ_1 and σ_3 (Figure 6.12).

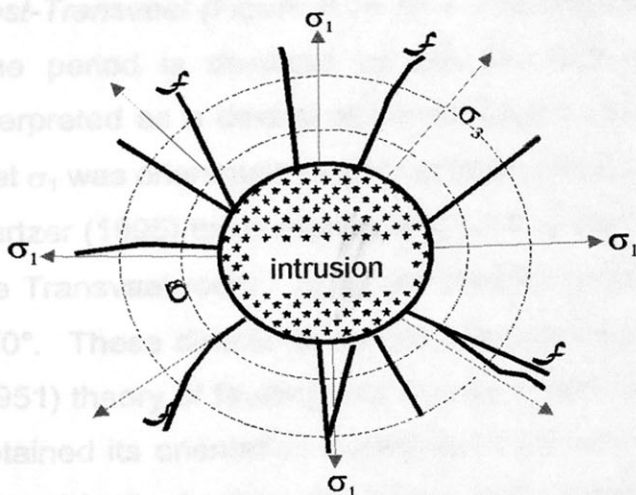


Figure 6.12. Stress directions related to the intrusion of a magmatic dome (modified from Weijermars, 1997)

Figure 6.13 is a geological map illustrating the distribution of faults present in the Bushveld Complex and surrounding areas. Rose diagrams of the orientation of the faults were generated according to various geological time periods. However, many faults are known to have been reactivated during geological history. Therefore, for each Bos area, rose diagrams of Age1 and Age2 faults are created. Age1 faults represent the first known activation age for the fault and Age2 faults represent any known reactivation ages for the faults.

Stress analysis for faults were impeded due to lack of data, or inconsistent interpretation in the literature. Therefore, in some cases more than one principal stress direction can be interpreted for the same fault during the same time period. Alternative interpretations are indicated with a light red colour on the rose diagram figures. Rose diagrams are discussed from the oldest time period, pre-Transvaal, to the youngest time period, post-Karoo.

6.3.1 Bos2

Fault Age1

Figure 6.14 shows a colour map of the faults for Age1 according to the various time periods they occur in, as well as a rose diagram of orientations of faults for each time period. Rose diagrams A through F show the stress orientation interpretation for each time period of Age1. They are interpreted as follows:

- *Pre-Transvaal (Figure 6.14 A)* - faults of this age in the Bos2 area include the Rietfontein fault system. This fault has been interpreted as a left-lateral strike-slip fault (Charlesworth et al., 1986) and therefore σ_1 will be orientated approximately 030° , σ_2 vertical, and σ_3 about 300° .
- *Post-Transvaal (Figure 6.14 B)* – The dominant faulting direction during this time period is depicted by the Rustenburg fault. The fault has been interpreted as a dextral strike-slip fault by Bumby (1997) and he suggested that σ_1 was orientated roughly at 340° , parallel to the D_2 direction proposed by Hartzler (1995) to be responsible for the interference fold pattern observed in the Transvaal rocks; σ_2 would then have been vertical and σ_3 orientated at 070° . These directions do not coincide with those predicted by Anderson's (1951) theory of faulting, but Bumby (1997) argued that the Rustenburg fault obtained its orientation during syn-Transvaal times when it was active as a normal fault. Another secondary fault pattern which is evident are the radial faults around the Johannesburg dome. It is possible that these faults reflect

Figure 6.13

Bosgis Fault Map

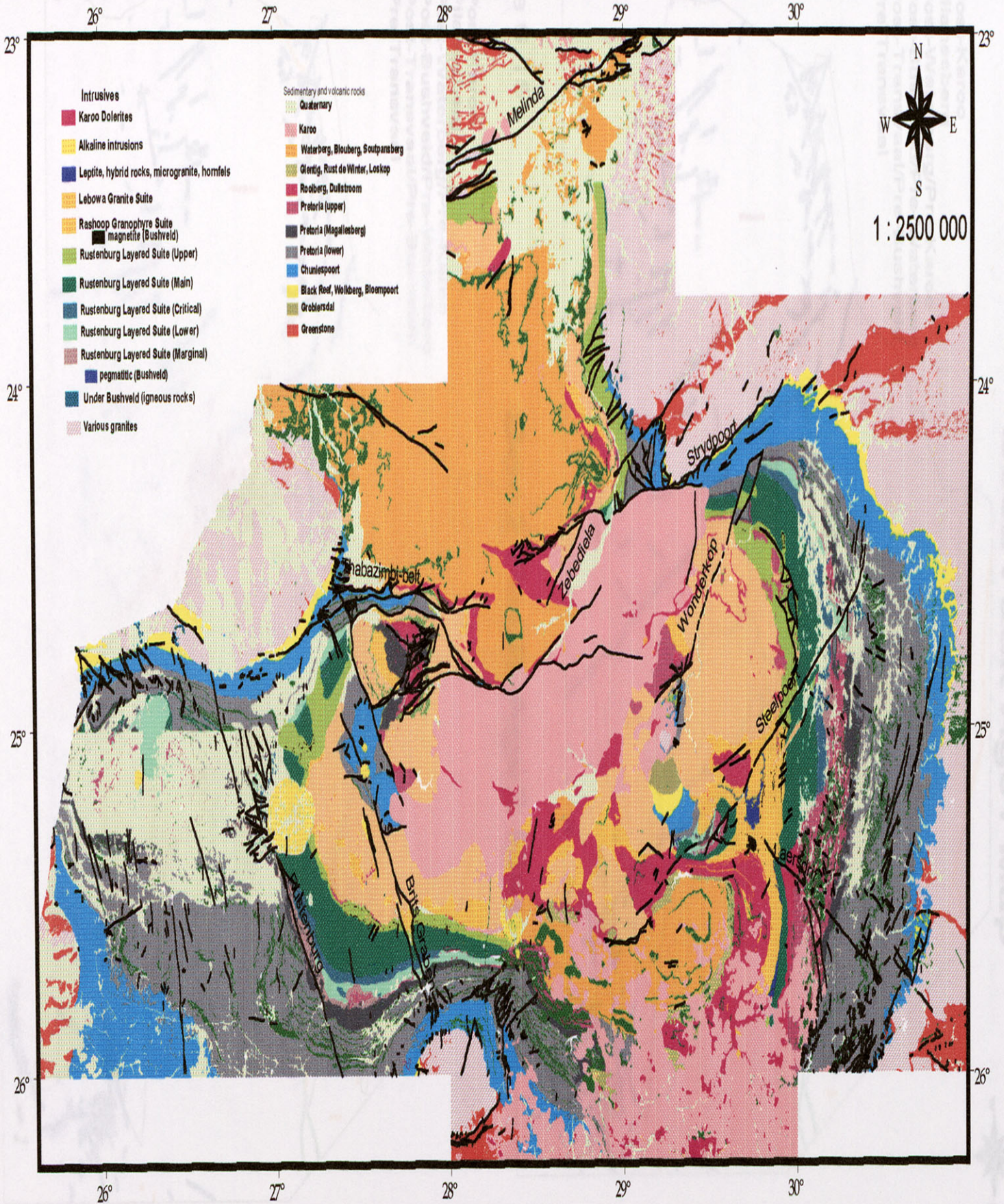


Figure 6.14

Bos2 Fault Age1 Map

- F  Post-Karoo
- E  Pilanesberg
- D  Post-Waterberg/Pre-Karoo
- C  Post-Bushveld/Pre-Waterberg
- B  Post-Transvaal/Pre-Bushveld
- A  Pre-Transvaal

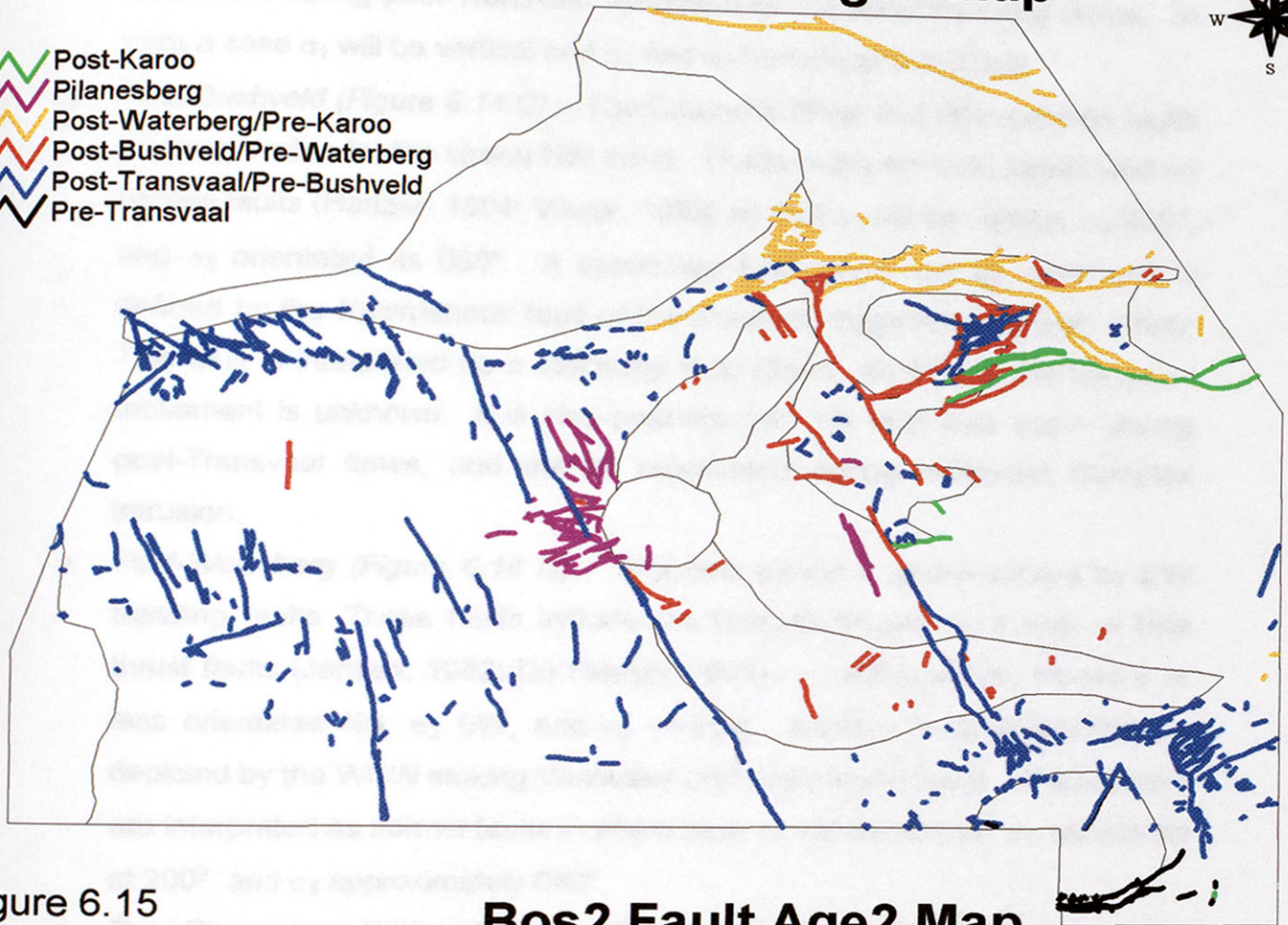
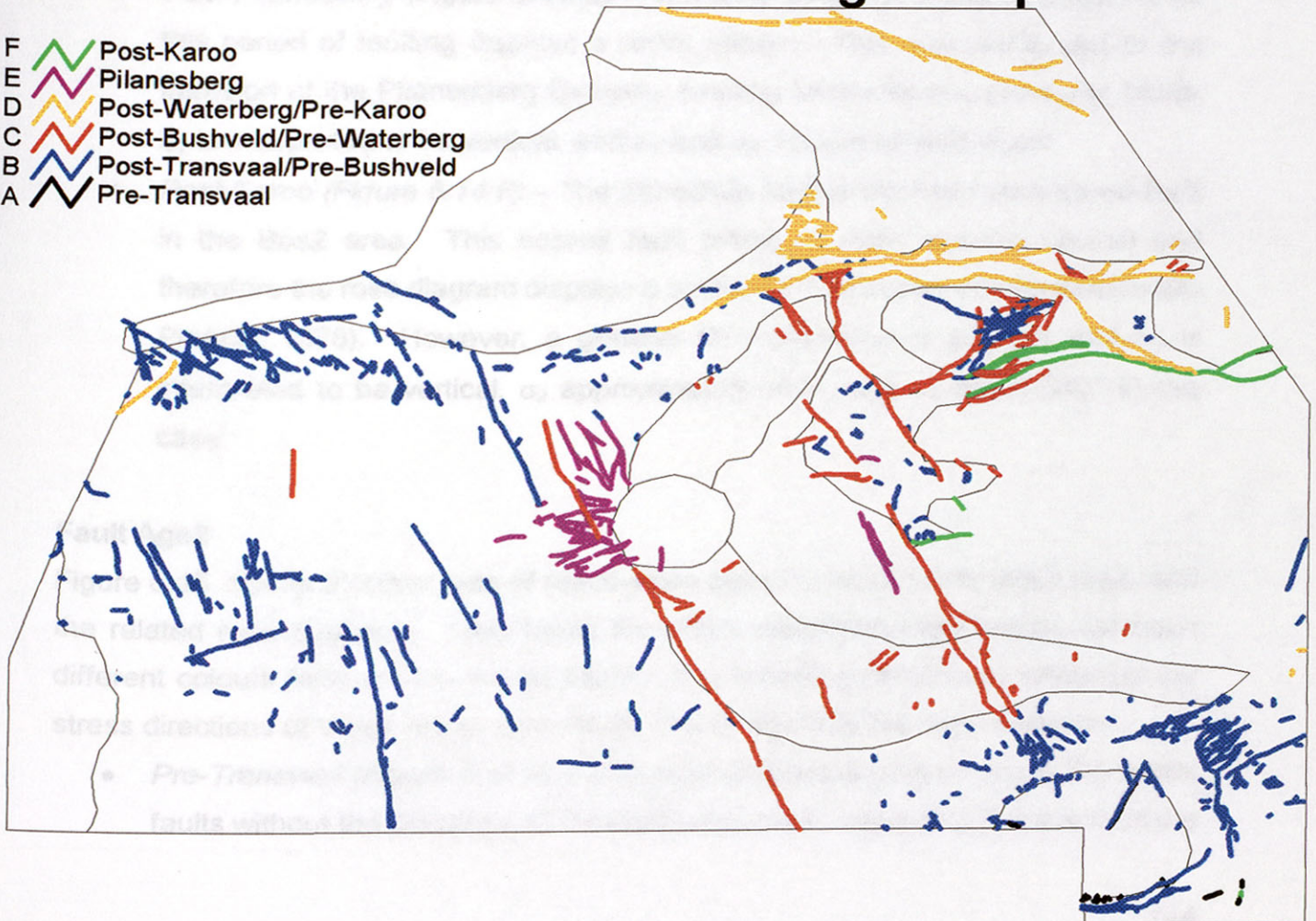


Figure 6.15

Bos2 Fault Age2 Map

- F  Post-Karoo
- E  Pilanesberg
- D  Post-Waterberg/Pre-Karoo
- C  Post-Bushveld/Pre-Waterberg
- B  Post-Transvaal/Pre-Bushveld
- A  Pre-Transvaal



movement during post-Transvaal upliftment of the Johannesburg dome. In such a case σ_1 will be vertical and σ_2 and σ_3 horizontal and equal.

- *Post-Bushveld (Figure 6.14 C)* – The Crocodile River and Brits Graben faults are responsible for the strong NW trend. These faults are both interpreted as normal faults (Hartzer, 1994; Visser, 1998) so that σ_1 will be vertical, σ_2 330°, and σ_3 orientated as 060°. A secondary ENE trend can be seen and is defined by the Kwarriehoek fault of the Rooiberg fragment (Hartzer, 1994). This fault is interpreted as a strike-slip fault (Stear, 1976), but the sense of movement is unknown. It is also possible that this fault was active during post-Transvaal times, and merely reactivated during Bushveld Complex intrusion.
- *Post-Waterberg (Figure 6.14 D)* – This time period is characterized by EW trending faults. These faults include the Bobbejaanwater and Belt of Hills thrust faults (Jansen, 1982; Du Plessis, 1991); σ_1 will therefore be more or less orientated NS, σ_2 EW, and σ_3 vertical. Another faulting direction is depicted by the WNW striking Vaalwater and Boschpoort faults. These faults are interpreted as normal faults in which case σ_1 will be vertical, σ_2 orientated at 290°, and σ_3 approximately 040°.
- *Post-Pilanesberg (Figure 6.14 E)* – The rose diagram of fault orientations for this period of faulting displays a radial pattern. This is probably due to the intrusion of the Pilanesberg Complex causing tensional and strike-slip faults. σ_2 is interpreted to be vertical, and σ_1 and σ_3 horizontal and equal.
- *Post-Karoo (Figure 6.14 F)* – The Zebediela fault is the main post-Karoo fault in the Bos2 area. This normal fault follows a fairly sinuous course and therefore the rose diagram displays a scattered distribution of orientations (Du Plessis, 1978). However, a general NE orientation is present and σ_1 is interpreted to be vertical, σ_2 approximately 060°, and σ_3 about 330° in this case.

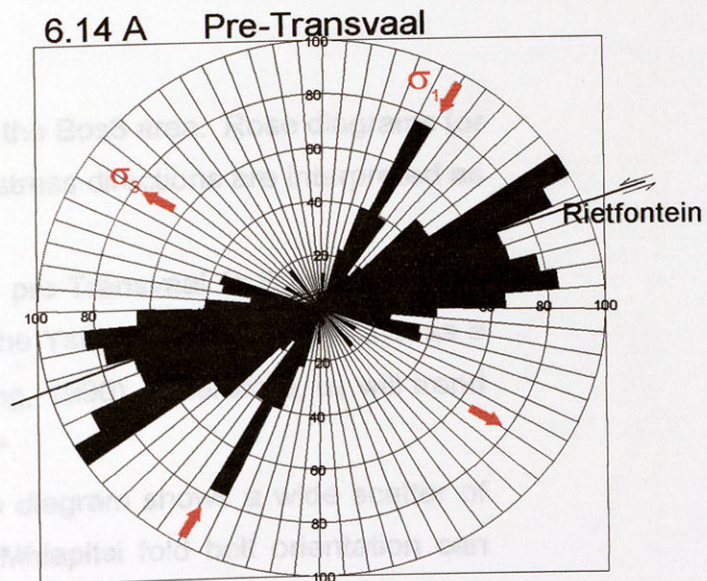
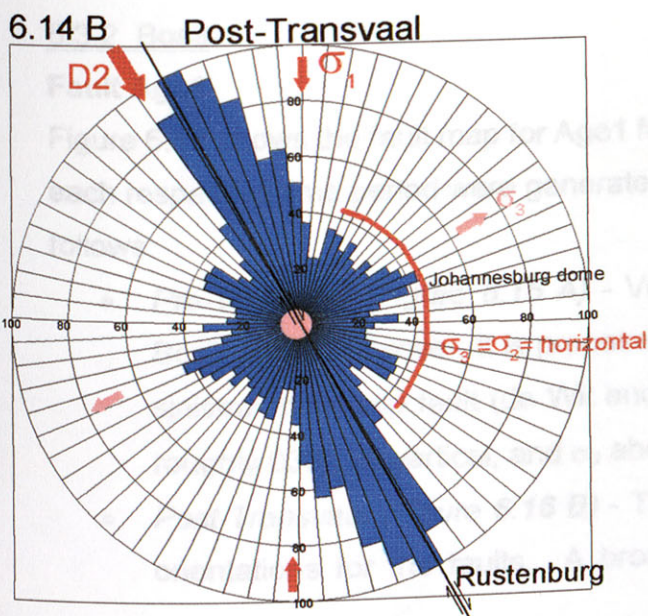
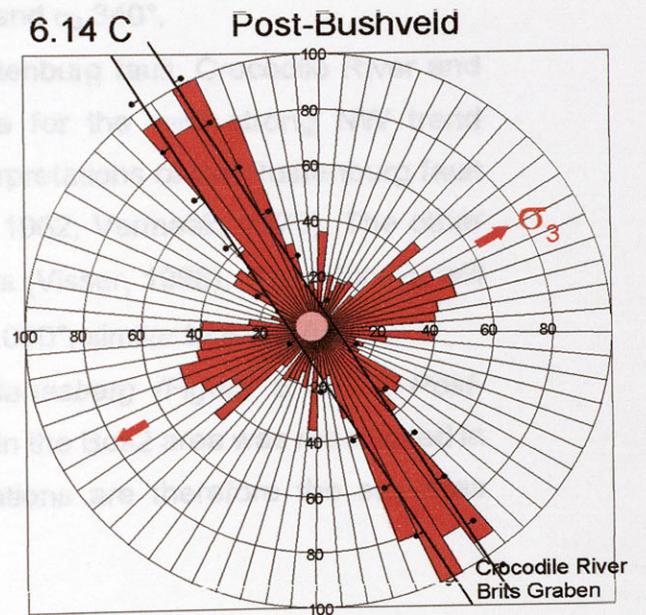
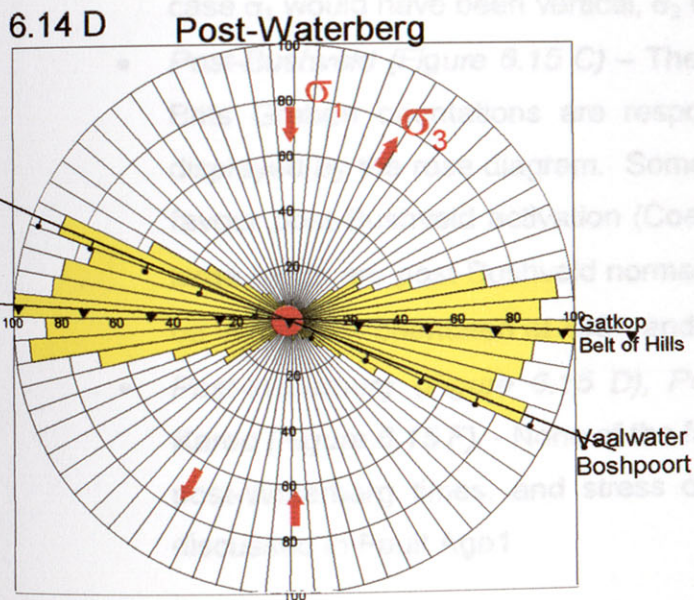
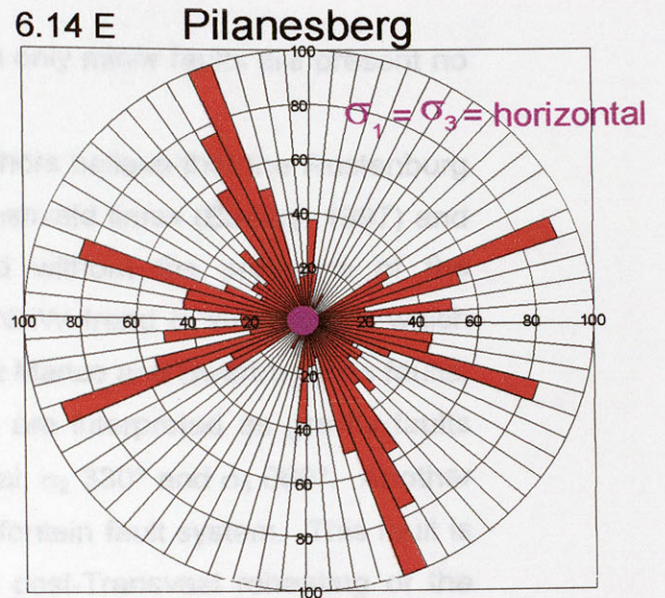
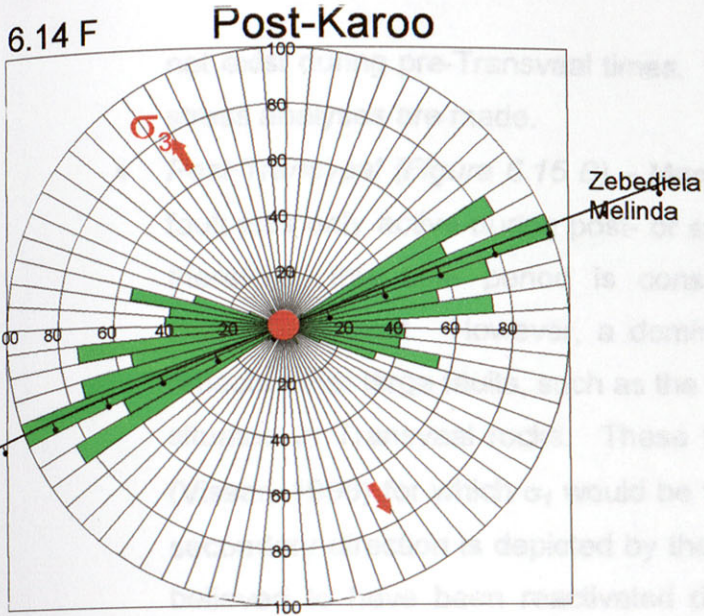
Fault Age2

Figure 6.15 shows a colour map of reactivation ages for faults in the Bos2 area, and the related rose diagrams. Only faults for which reactivation are known will have different colours from the Fault Age1 faults. The following discussion interprets the stress directions of these reactivation faults as portrayed by the rose diagrams.

- *Pre-Transvaal (Figure 6.15 A)* – This rose diagram displays the pre-Transvaal faults without the presence of the Rietfontein fault, assuming that the fault did

Interpretation of stress directions of Bos2 Fault Age1

University of Pretoria etd - Greyvenstejn, R.M (2001)



not exist during pre-Transvaal times. Since only minor faults are present no stress analyses are made.

- *Post-Transvaal (Figure 6.15 B)* – Many authors believe that the Rustenburg fault was only active during post- or syn-Bushveld times (Bumby, 1997) and therefore, this time period is considered without the presence of the Rustenburg fault. However, a dominant NNW trend is still present which reflects other large faults, such as the Groot Marico and Swartruggens faults, situated in Transvaal rocks. These faults are interpreted as gravity faults (Visser, 1998) for which σ_1 would be vertical, σ_2 330° and σ_3 060°. Another secondary direction is depicted by the Rietfontein fault system. This fault is believed to have been reactivated during post-Transvaal reheating of the Johannesburg dome as a normal fault (Charlesworth et al., 1986). In this case σ_1 would have been vertical, σ_2 070° and σ_3 340°.
- *Post-Bushveld (Figure 6.15 C)* – The Rustenburg fault, Crocodile River and Brits Graben orientations are responsible for the very strong NW trend displayed by the rose diagram. Some interpretations of the Rustenburg fault favour post-Bushveld activation (Coertze, 1962; Vermaak, 1970). The other large faults are post-Bushveld normal faults (Visser, 1998). Therefore σ_1 will be vertical, σ_2 orientated at 330°, and σ_3 at 060°, similar to Fault Age 1.
- *Post-Waterberg (Figure 6.15 D), Post-Pilanesberg (Figure 6.15 E), Post-Karoo (Figure 6.15 F)*, - None of the faults in the Bos2 area was reactivated in post-Waterberg times, and stress orientations are therefore the same as discussed in Fault Age1.

6.3.2 Bos3

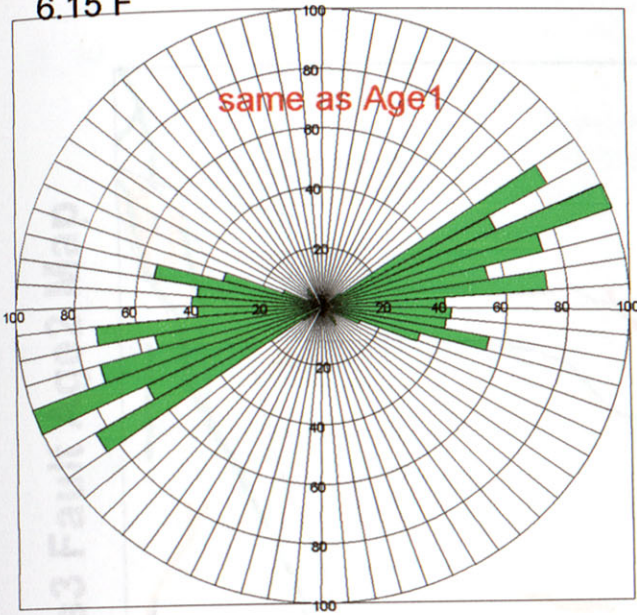
Fault Age1

Figure 6.16 shows the fault map for Age1 faults of the Bos3 area. Rose diagrams for each respective time period were generated, and stress directions are interpreted as follows:

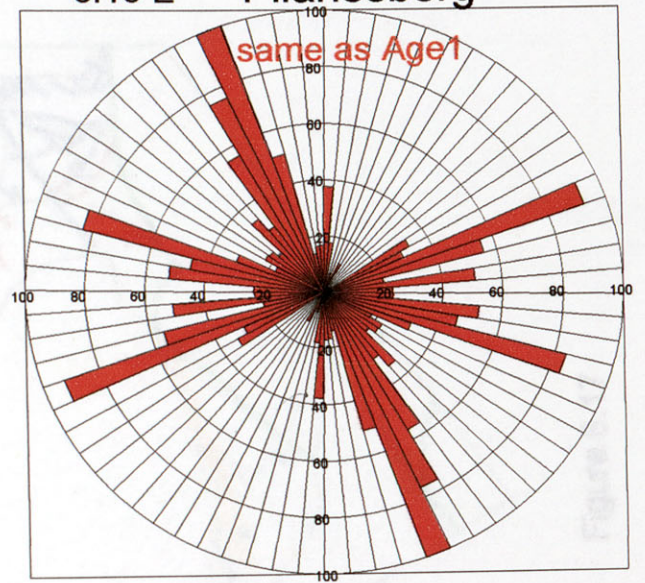
- *Pre-Transvaal (Figure 6.16 A)* - Very few pre-Transvaal faults occur in the Bos3 area. However, it is proposed that the Ysterberg fault was active as a sinistral strike-slip fault (de Wit and Roering, 1990). Therefore, σ_1 will trend roughly 030°, σ_2 vertical, and σ_3 about 300°.
- *Post-Transvaal (Figure 6.16 B)* - The rose diagram shows a wide scatter of orientations for the faults. A broad NE Mhlapitsi fold belt orientation can

Interpretation of stress directions of Bos2 Fault Age2

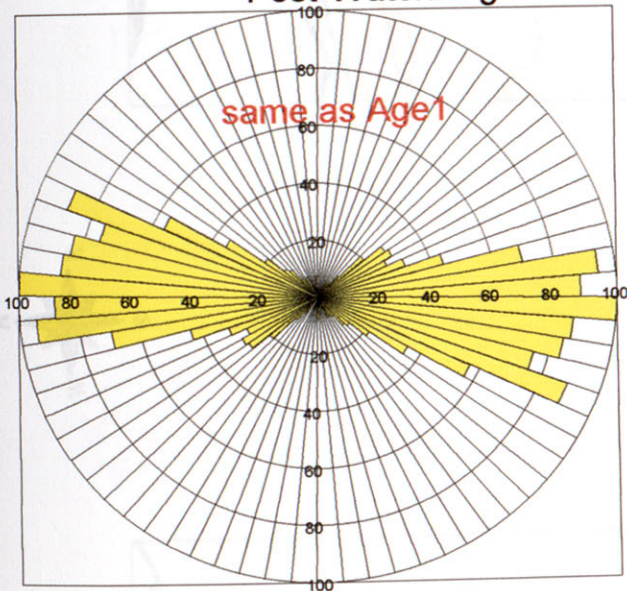
6.15 F Post-Karoo



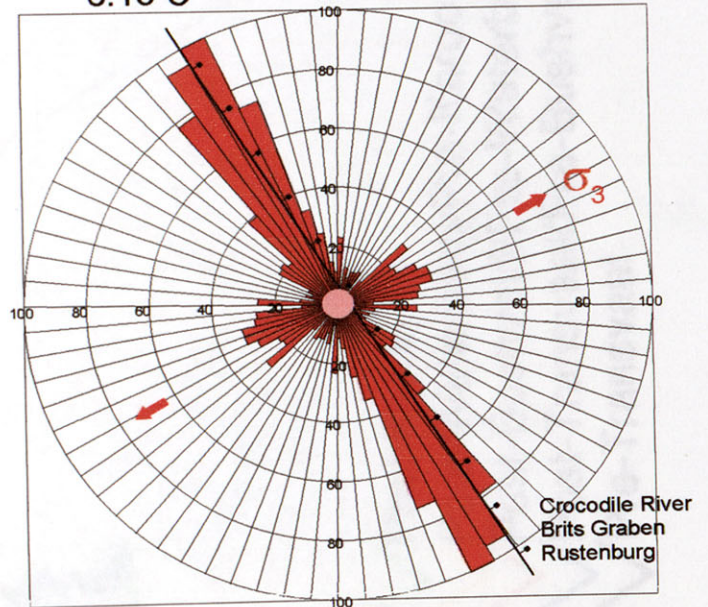
6.15 E Pilanesberg



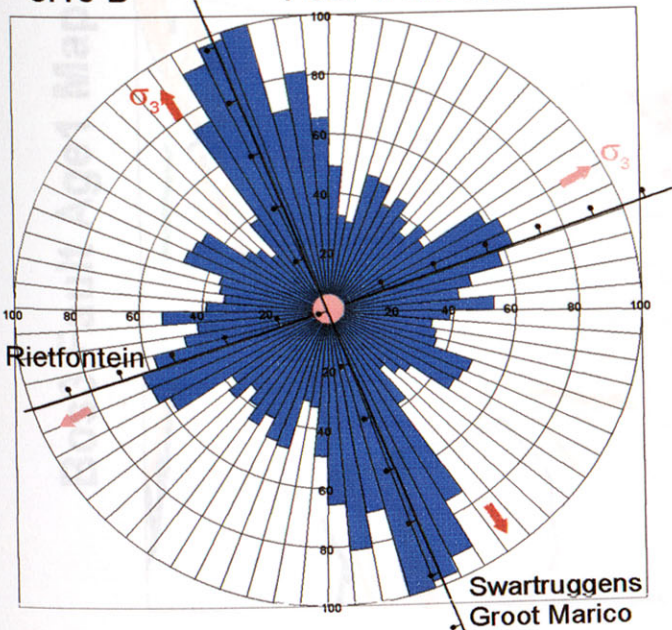
6.15 D Post-Waterberg



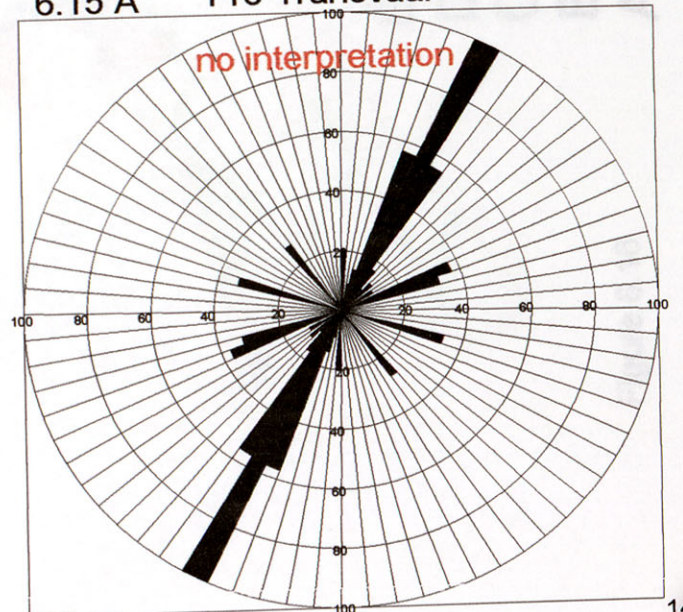
6.15 C Post-Bushveld



6.15 B Post-Transvaal



6.15 A Pre-Transvaal





Bos3 Fault Age1 Map








Figure 6.16

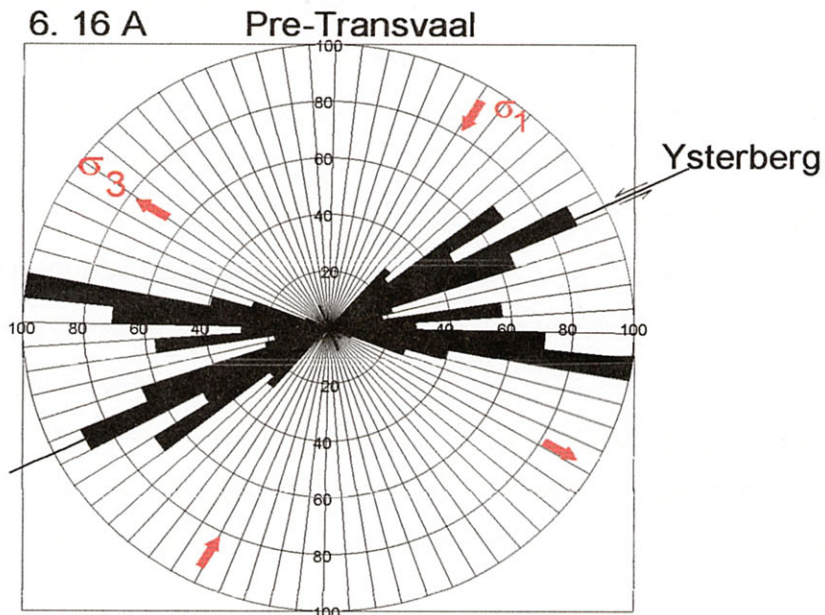
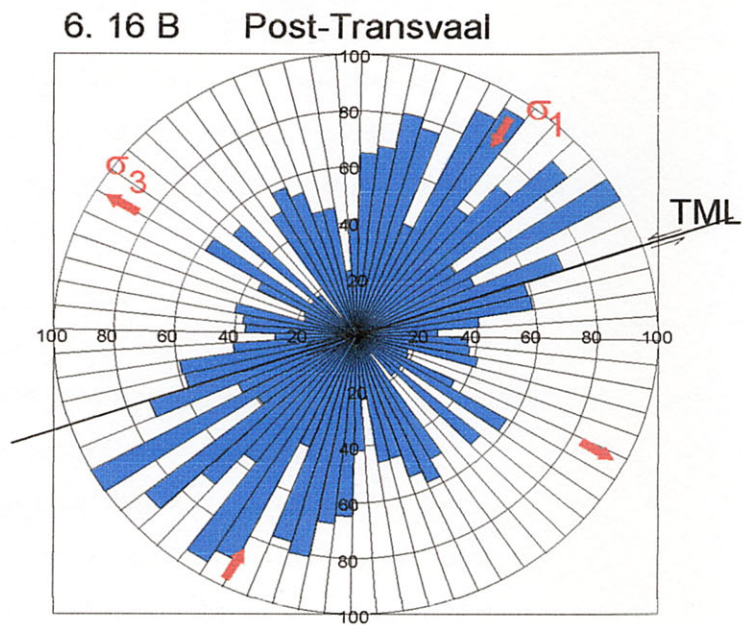
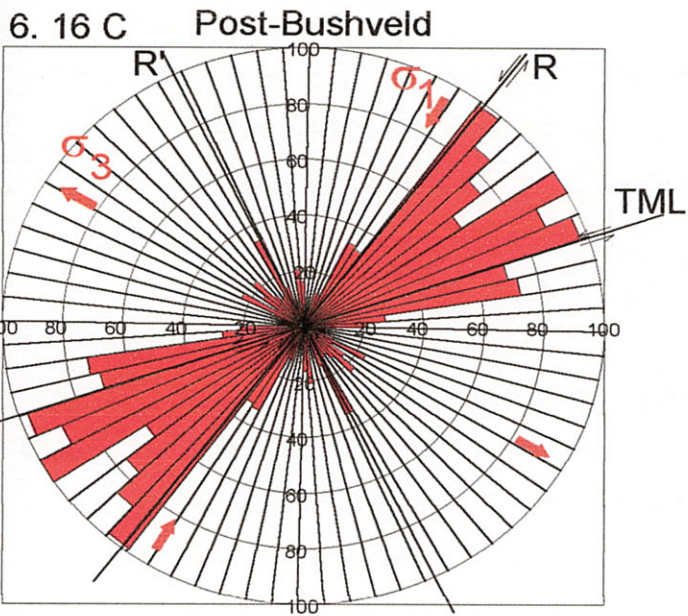
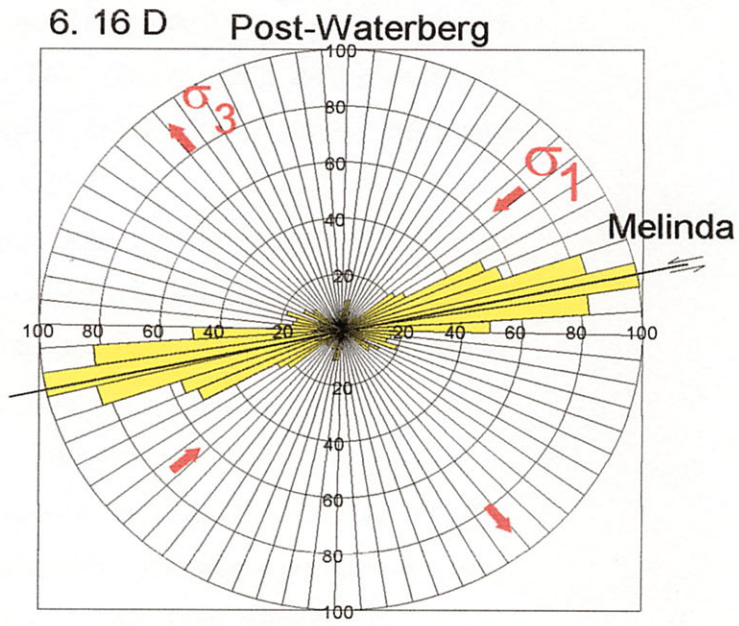
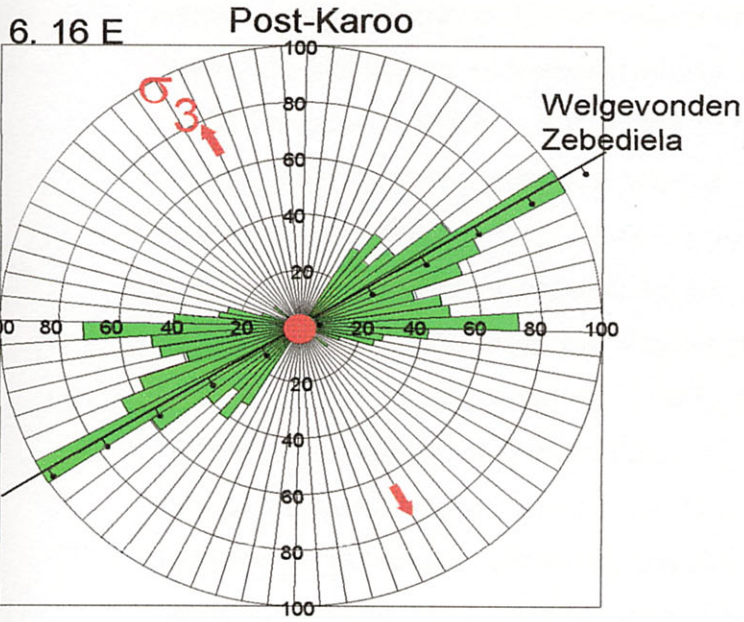
Bos3 Fault Age2 Map



Figure 6.17

- E  Post Karoo
- D  Post-Waterberg/Pre-Karoo
- C  Post-Bushveld/Pre-Waterberg
- B  Post-Transvaal/Pre-Bushveld
- A  Pre-Transvaal

Interpretation of stress orientations for Bos3 Age1



however be recognized. Other main faults could be conjugate strike-slip faults related to left-lateral movement along the TML (Du Plessis and Walraven, 1990; Potgieter, 1992). For these conjugate strike-slip faults σ_1 will trend roughly 030° , σ_2 vertical, and σ_3 orientated at 330° .

- *Post-Bushveld (Figure 6.16 C)* - The northern lobe of the Bushveld Complex contains several NE orientated faults as can be seen by the orientations displayed on the rose diagram. These faults are interpreted as Riedel shears related to left-lateral movement along the TML (Du Plessis, 1991). σ_1 will therefore be orientated around 030° , σ_2 vertical, and σ_3 at 300° .
- *Post-Waterberg (Figure 6.16 D)* - The Melinda fault is responsible for the dominant ENE trend depicted by the rose diagram. The Melinda fault is a left-lateral strike-slip fault (Brandl and Reimold, 1990) and would have been caused by a σ_1 orientated approximately 050° , a vertical σ_2 , and a σ_3 trending 320° .
- *Post-Karoo (Figure 6.16 E)* - the dominant NE trend is caused by the Zebediela and Welgevonden faults. These normal faults (Du Plessis, 1978) would have been caused by a vertical σ_1 , σ_2 directed 070° , and σ_3 directed 340° .

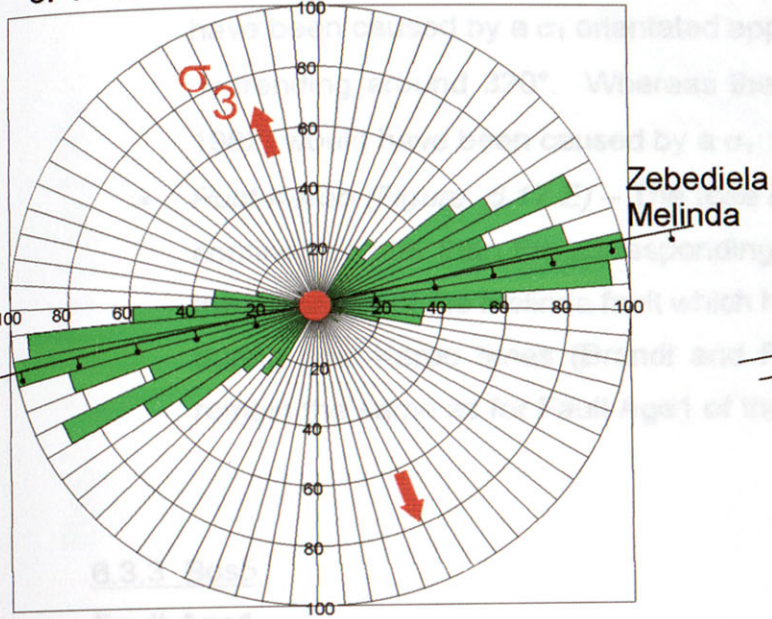
Fault Age2

Figures 6.17 A-E shows the reactivation ages of the Bos3 faults where known. The stress directions for the reactivation histories are interpreted as follows:

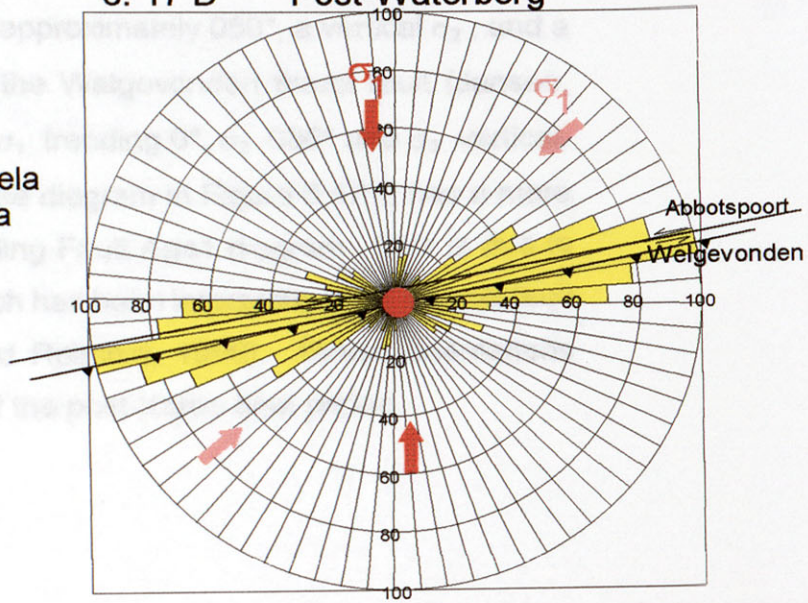
- *Pre-Transvaal (Figure 6.17 A)* – If the Ysterberg fault was not active during pre-Transvaal times, the orientation of other supposedly pre-Transvaal faults are depicted by Figure 6.17 A. It is uncertain whether these are truly of pre-Transvaal age or if they are younger. Also, since only minor faults are present no stress orientations were interpreted.
- *Syn-Transvaal (Figure 6.17 B)* - This time period is characterized by the post-Chuniespoort/pre-Pretoria reactivation of the Ysterberg fault. The fault is suggested to have been a thrust fault (Potgieter, 1992) and therefore, σ_1 would have been orientated at 330° , σ_2 060° , and σ_3 vertically.
- *Post-Bushveld (Figure 6.17 C)* – Stress orientations for this time period is the same as Fault Age1(Figure 6.16 C).
- *Post-Waterberg (Figure 6.17 D)* – The main faulting directions of this time period are depicted by the Abbotspoort and Welgevonden faults. The possibly left-lateral Abbotspoort fault (McCourt and Vearncombe, 1992) would

Interpretation of stress orientations for Bos3 Age2

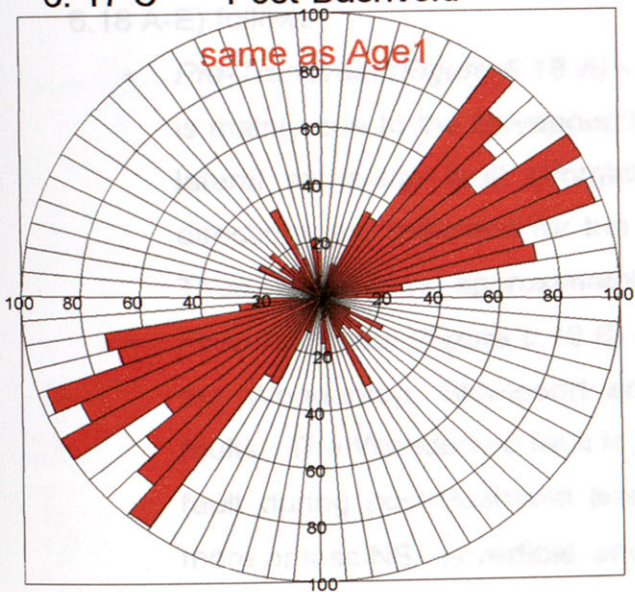
6. 17 E Post-Karoo



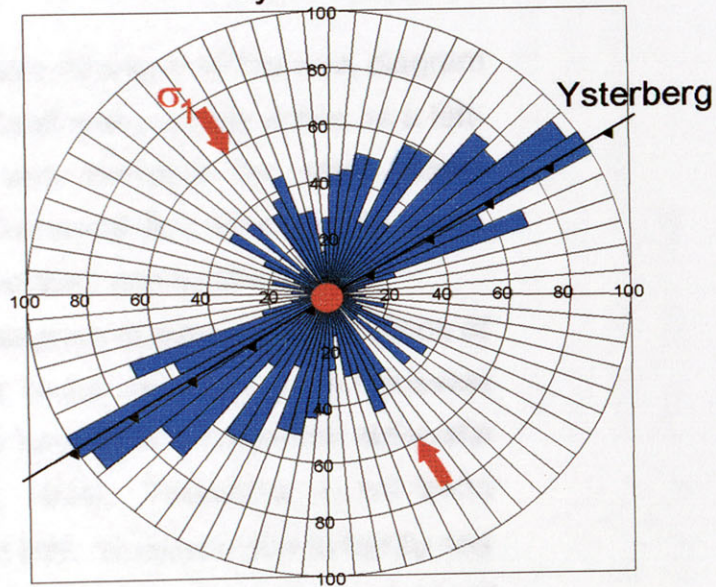
6. 17 D Post-Waterberg



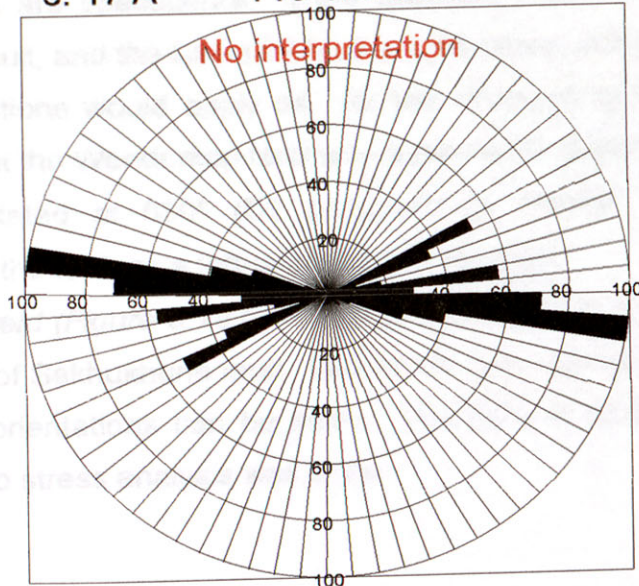
6. 17 C Post-Bushveld



6. 17 B Syn-Transvaal



6. 17 A Pre-Transvaal



have been caused by a σ_1 orientated approximately 050° , a vertical σ_2 , and a σ_3 trending around 320° . Whereas the Welgevonden thrust fault (Jansen, 1982) would have been caused by a σ_1 trending 0° , σ_2 080° and σ_3 vertical.

- *Post-Karoo (Figure 6.17 E)* – The rose diagram in Figure 6.17 E has a more confined scatter than the corresponding Fault Age1 diagram. This is due to the presence of the Melinda fault which has been interpreted as a normal fault during post-Karoo times (Brandl and Reimold, 1990). Stress orientations remain the same as for Fault Age1 of the post-Karoo time period.

6.3.3 Bos5

Fault Age1

Figure 6.18 shows the fault map and rose diagrams of fault orientations of the Bos5 area. A discussion of the stress directions derived from the rose diagrams (Figures 6.18 A-E) follows:

- *Pre-Transvaal (Figure 6.18 A)* – The dominant direction on the rose diagram is mainly due to the Strydpoort fault. This fault was possibly active as a left-lateral strike-slip fault (Potgieter, 1992) and therefore the same stress directions as indicated for the other pre-Transvaal Bos areas would apply. Thus, σ_1 will trend approximately 020° , σ_2 vertical, and σ_3 trends 290° .
- *Post-Transvaal (Figure 6.18 B)* – The rose diagram depicts the orientations of the Wonderkop, Steelpoort and Laersdrif faults as active post-Transvaal faults. The Wonderkop fault is proposed to have been a left-lateral strike-slip fault during post-Bushveld times (Hartzer, 1994). Therefore, σ_1 will trend more or less NS, σ_2 vertical, and σ_3 directed EW. However, due to hardly any published research on the Steelpoort and Laersdrif faults, stress analyses of these faults are speculative. If the Steelpoort fault was also a left-lateral strike-slip fault, and the Laersdrif fault a right-lateral strike-slip fault, the same stress directions would apply as for the Wonderkop fault. However, it is possible that the Wonderkop fault was a pre-existing weakness, in which case a σ_1 orientated at 030° (D2 proposed by Hartzer, 1994) would have reactivated the fault as a left-lateral strike-slip fault.
- *Post-Bushveld (Figure 6.18 C)* – The rose diagram is a representation of the orientation of Sekhukhune fault. Due to the sinuous nature of the fault a wide scatter of orientations can be seen. The type of faulting is unknown and therefore no stress analysis was done.

Bos5 faults Age1 Map

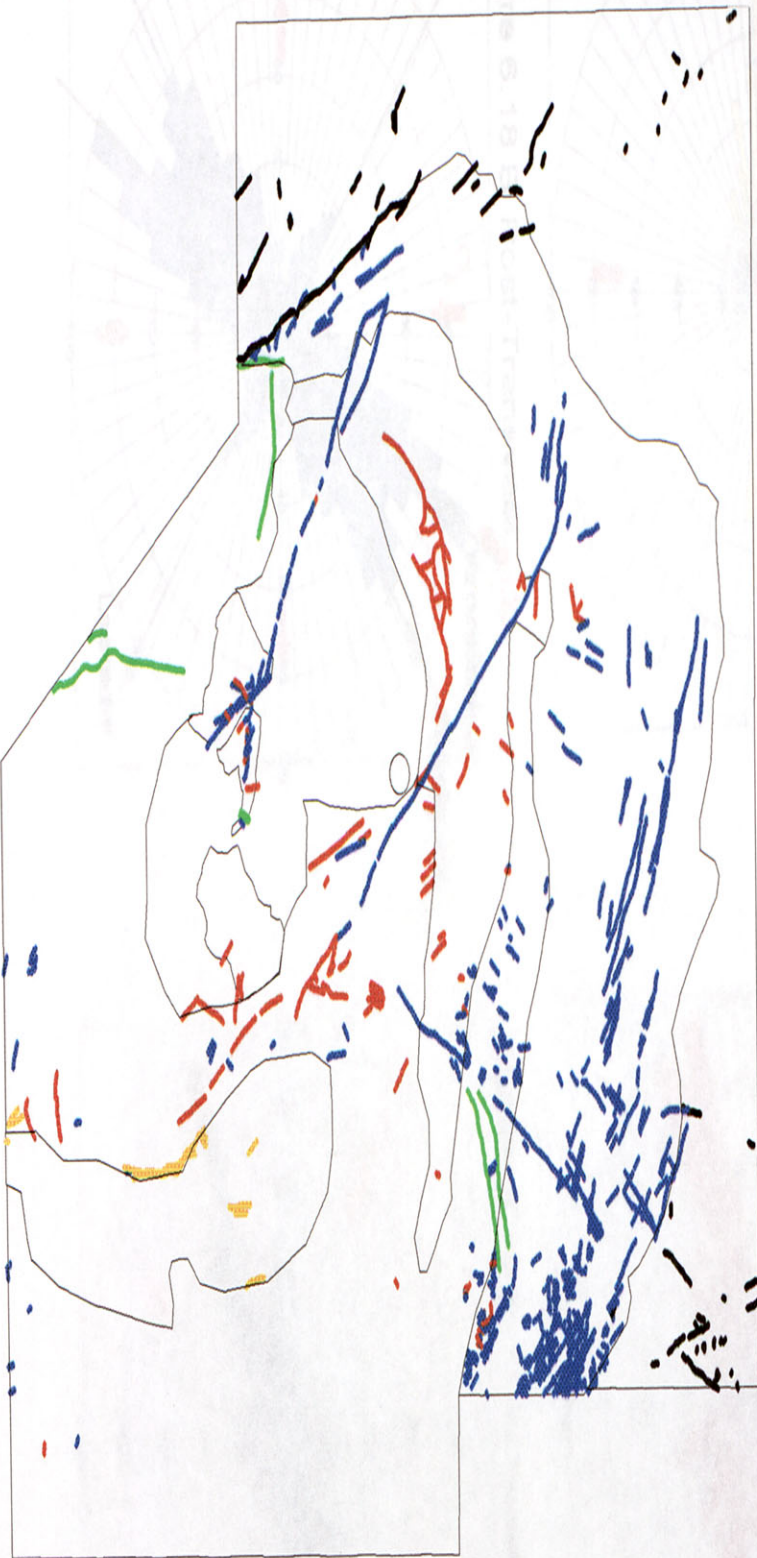


Figure 6.18

Bos5 faults Age2 Map

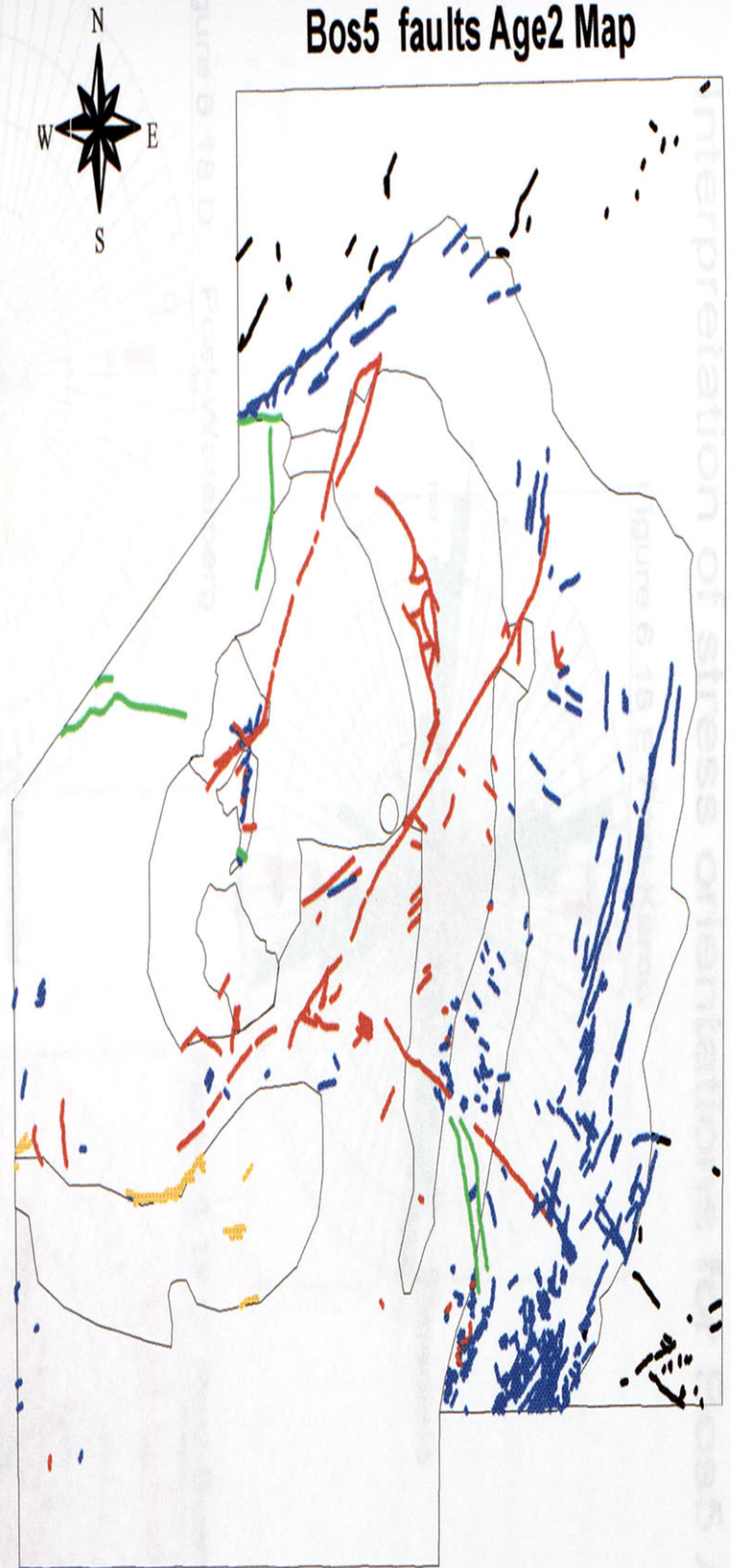


Figure 6.19

- E  Post Karoo
- D  Post Waterberg/Pre Karoo
- C  Post Bushveld/Pre Waterberg
- B  Post Transvaal/Pre Bushveld
- A  Pre Transvaal

Interpretation of stress orientations for Bos5 Age1

Figure 6.18 E Post-Karoo

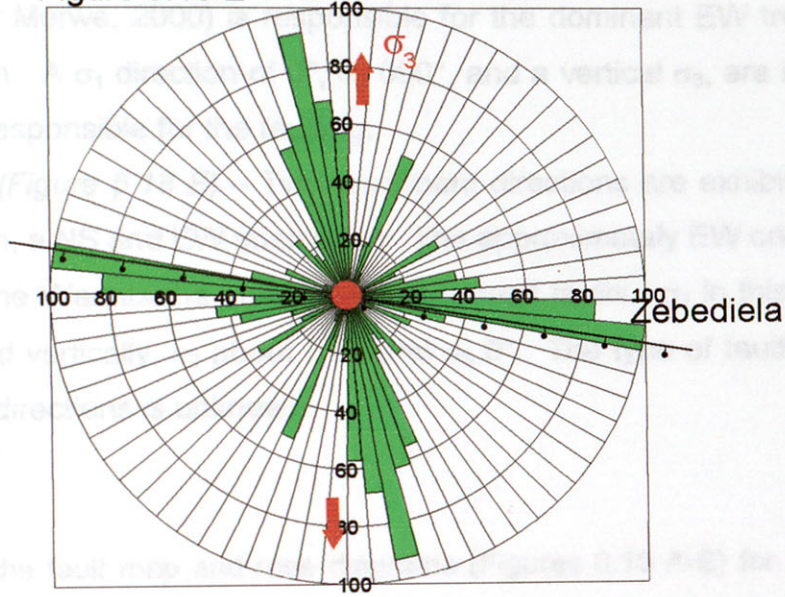


Figure 6.18 D Post-Waterberg

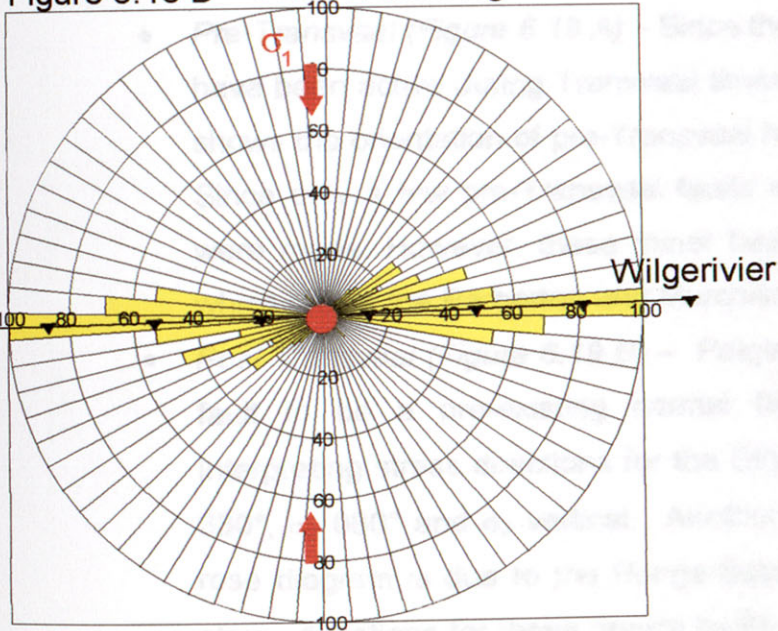


Figure 6.18 C Post-Bushveld

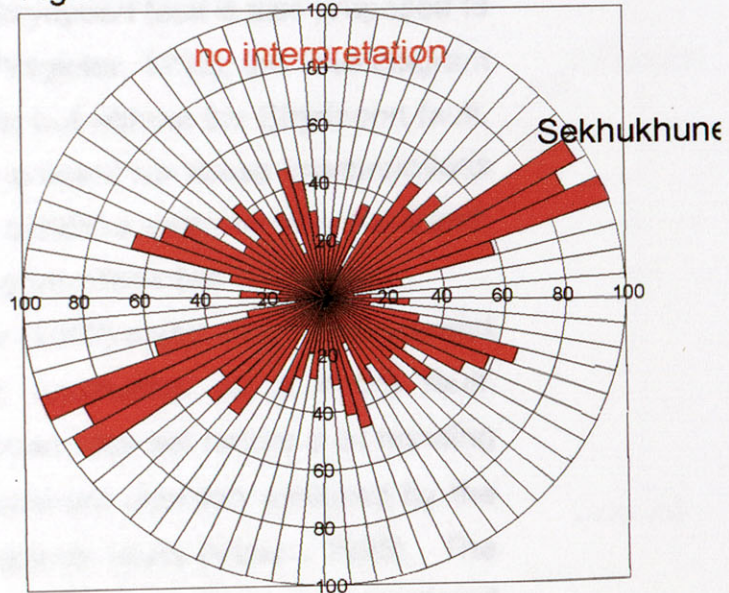


Figure 6.18 B Post-Transvaal

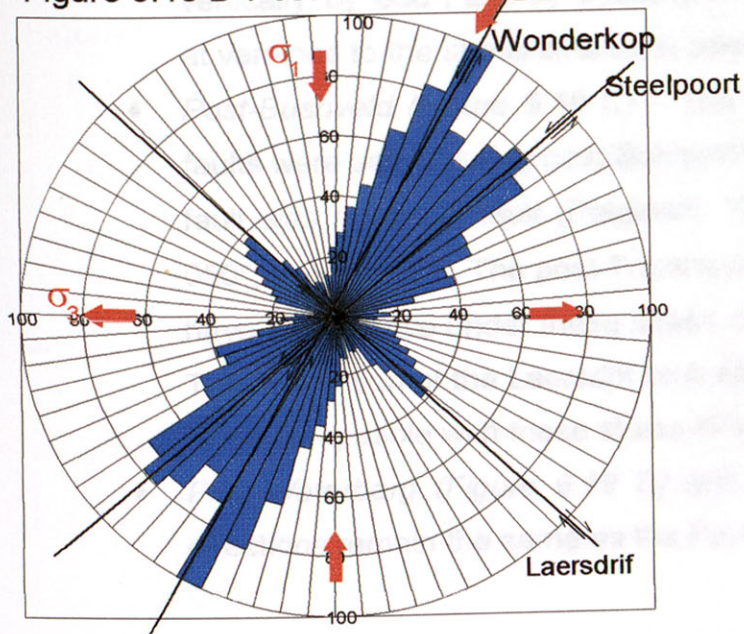
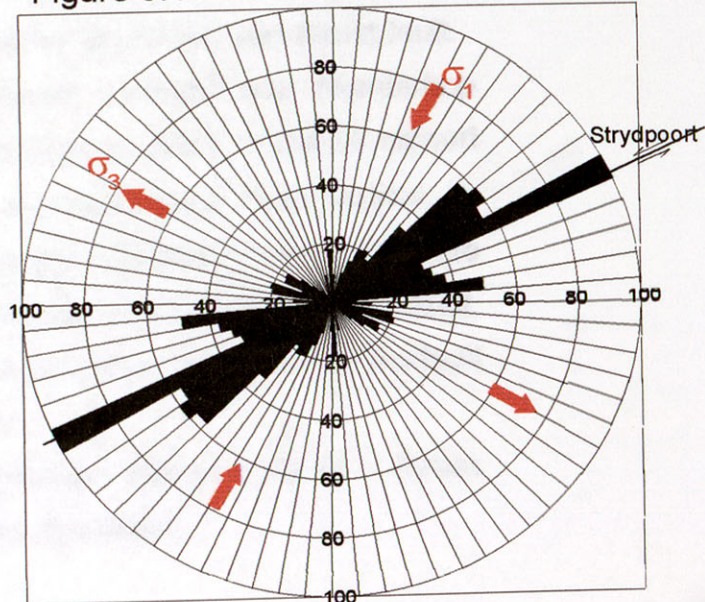


Figure 6.18 A Pre-Transvaal



- *Post-Waterberg (Figure 6.18 D)* – The Wilgerivier thrust fault (Van der Neut and Van der Merwe, 2000) is responsible for the dominant EW trend in the rose diagram. A σ_1 direction of 0° , σ_2 090° , and a vertical σ_3 , are inferred to have been responsible for the faulting.
- *Post-Karoo (Figure 6.18 E)* – Two prominent directions are exhibited by the rose diagram, a NS and EW orientation. The approximately EW orientation is the due to the Warmbaths and Zebediela normal faults. σ_1 in this case will be orientated vertically, σ_2 about EW, and σ_3 0° . The type of faulting for the NS faulting directions is unknown.

Fault Age2

Figure 6.19 shows the fault map and rose diagrams (Figures 6.19 A-E) for reactivated faults in the Bos5 area. Stress directions for these faults are interpreted as follows:

- *Pre-Transvaal (Figure 6.19 A)* – Since the Strydpoort fault is also proposed to have been active during Transvaal times (Potgieter, 1992), the rose diagram shows the orientation of pre-Transvaal faults but without the Strydpoort fault. Since only a few pre-Transvaal faults are present no stress interpretations were made. However, these minor faults exhibit a more or less NE trend, which reflect the Barberton and Murchison greenstone belt directions.
- *Post-Transvaal (Figure 6.19 B)* – Potgieter (1992) suggested the Strydpoort fault to be a pre-existing normal fault, reactivated as a thrust fault. Interpreting stress directions for the Strydpoort fault will render a σ_1 trending 330° , σ_2 060° and σ_3 vertical. Another dominant direction exhibited by the rose diagram is due to the Penge-Sabie gravity faults (Visser, 1998). The stress directions for these gravity faults are interpreted to be a σ_1 , orientated vertically, σ_2 030° , and σ_3 trending 300° . These stress directions are clearly at variance to the stress directions interpreted for the Strydpoort thrust fault.
- *Post-Bushveld (Figure 6.19 C)* – The Steelpoort, Laersdrif and Wonderkop faults were active during post-Bushveld times (Visser, 1998). If the Steelpoort fault was a normal fault (Potgieter, 1992), σ_1 would have been vertical, σ_2 050° , and σ_3 320° . The post-Transvaal strike-slip Wonderkop fault could also have been active under these stress directions as a reactivated normal fault. The orientation of the Laersdrif fault either as a normal or as a strike-slip fault is not compatible with these stress directions.
- *Post-Waterberg (Figure 6.19 D) and Post-Karoo (Figure 6.19 E)* - Stress directions remain the same as the Fault Age1 directions.

Interpretation of stress orientations for Bos5 Age2

Figure 6.19 E Post-Karoo

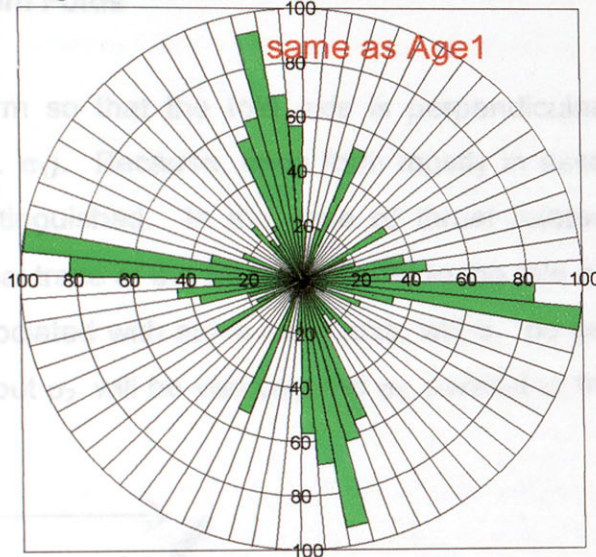


Figure 6.19 D Post-Waterberg

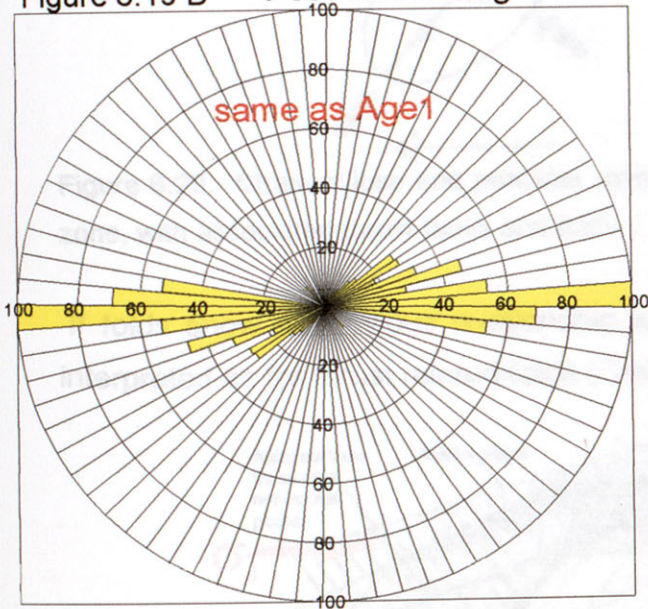


Figure 6.19 C Post-Bushveld

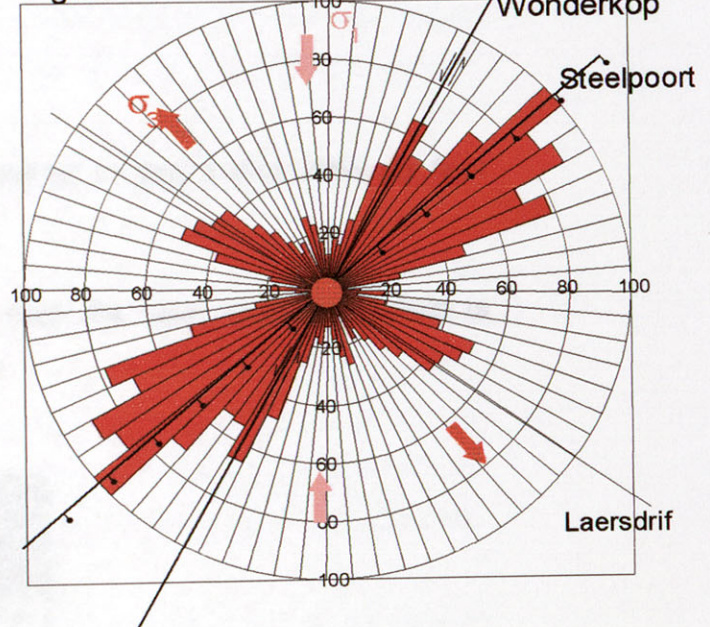


Figure 6.19 B Post-Transvaal

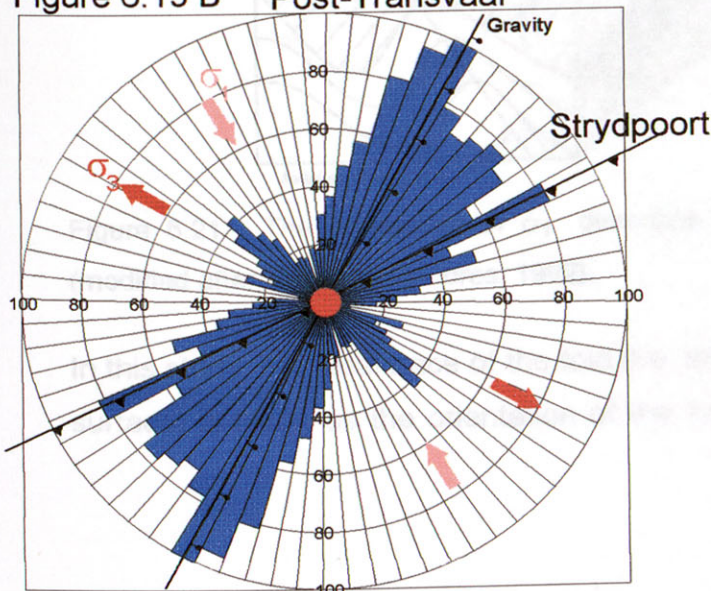
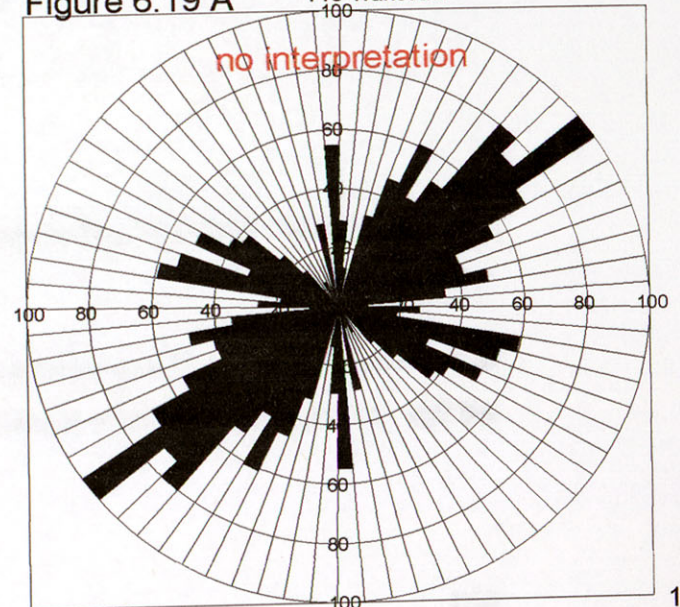


Figure 6.19 A Pre-Transvaal



6.4 Stress analysis from Folds

Folds will generally form so that the fold axis is perpendicular to the maximum compressive stress (i.e. σ_1). Because, folds form mostly in association with faults two cases may be distinguished. In the case of thrust related folds, σ_1 will be perpendicular to the axial trace of the fold, σ_2 parallel to the fold axis, and σ_3 vertical. However, for folds associated with strike-slip faults, σ_1 will be perpendicular to the axial trace of the fold, but σ_2 will be vertical, and σ_3 parallel to the fold axis (Figure 6.20).

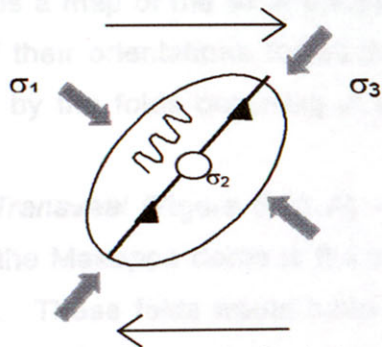


Figure 6.20. Strain ellipse and principal stress directions for an ideal dextral strike-slip fault zone, with associated thrust faults and folds.

If folds show no obvious relationship to faults, then the causative stress field is interpreted as for thrust related folds (Figure 6.21).

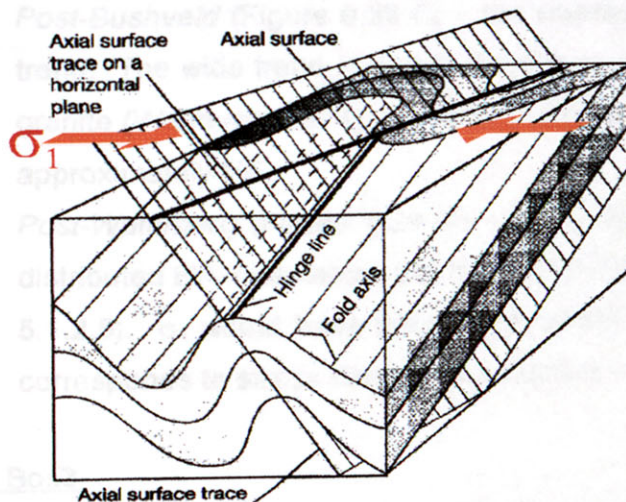


Figure 6.21. The orientation of σ_1 directions as interpreted for folds during this study (modified after Twiss and Moores, 1992).

In this study, the axial trace of the fold (i.e. the intersection of the axial plane with the surface) is taken as the orientation of the fold (Figure 6.21). Therefore, σ_1 will be

horizontal for both thrust and strike-slip fault related folds and also for non-fault related folds. Only σ_1 directions are mentioned and indicated on the figures.

Axial traces of folds occurring in the Bushveld Complex and surrounding areas are illustrated in Figure 6.22. Stress orientations for the folds are interpreted according to the Bos area they occur in, and according to the various time periods during which the folds formed.

6.4.1 Bos2

Figure 6.23 is a map of the axial traces of folds as well as the corresponding rose diagrams of their orientations for each folding period. Four fold generations are represented by the folds occurring in the Bos2 area, and they are interpreted as follows:

- *Pre-Transvaal* (Figure 6.23 A) – Some authors believe (e.g. Hunter, 1974) that the Makoppa dome is the product of NW and NE trending interference folds. These folds would have been caused by σ_1 orientated NE and NW respectively.
- *Post-Transvaal* (Figure 6.23 B) – The same two folding directions as discussed above characterizes the post-Transvaal folds, especially the folds present in the Transvaal inliers (Hartzer, 1995). These folds are also the response to σ_1 orientated NE (D1) and NW (D2) respectively, (Hartzer, 1995).
- *Post-Bushveld* (Figure 6.23 C) – the orientation of folds define a broad NW trend. The wide trend is due to the sinuous folds contained in the Bushveld granite (Walraven, 1974). σ_1 for this folding event is inferred to be orientated approximately NE.
- *Post-Waterberg* (Figure 6.23 D) – these folds are orientated in a narrowly distributed EW orientation, but the age of the folds are not well constraint (see 5.1.2.5). σ_1 would have been directed NS during this folding event, which corresponds to stress directions analysed for faults during this time period.

6.4.2 Bos3

The orientations of the axial traces of the few folds present in the Bos3 area are illustrated in Figure 6.24 and the corresponding rose diagram. A few small NE trending Mhlapitsi folds occur in the Transvaal rocks, for which σ_1 trends 320° . The principal stress direction for the formation of the post-Waterberg folds is inferred to be a NS directed σ_1 .

Figure 6.22

Bosgis Fold Map

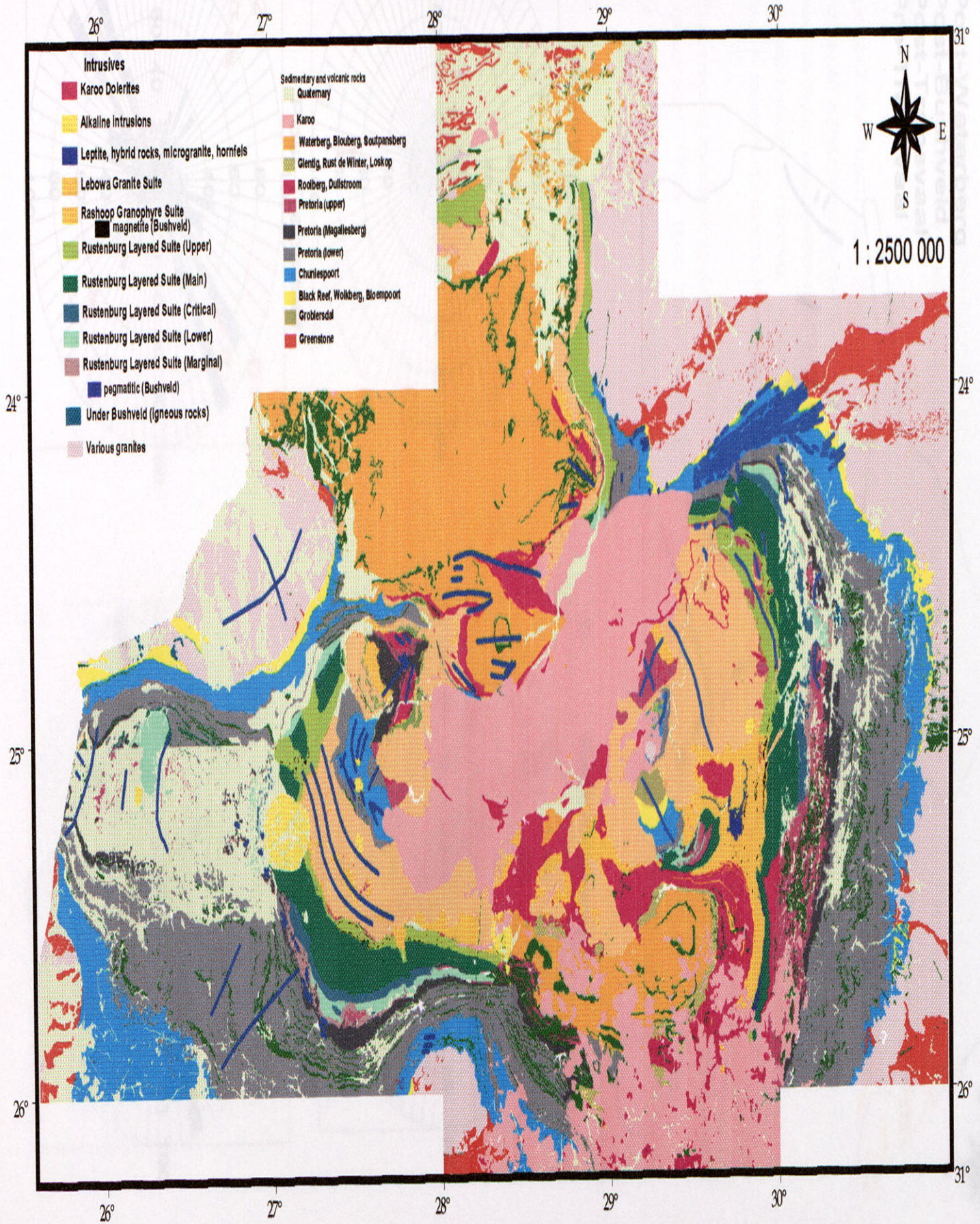
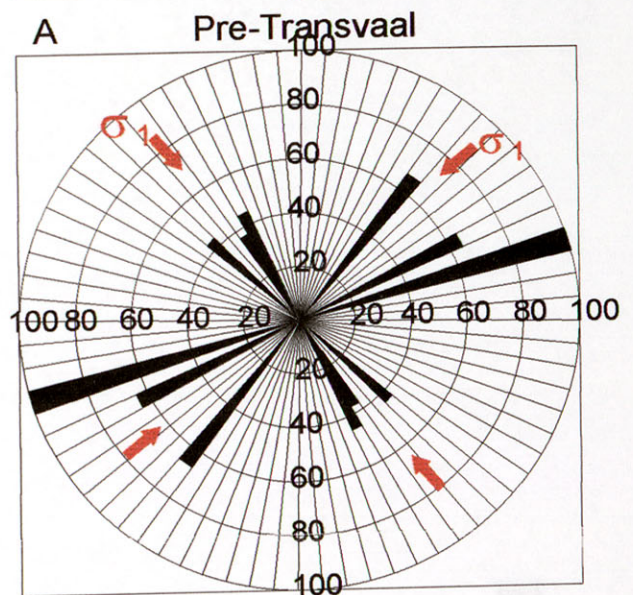
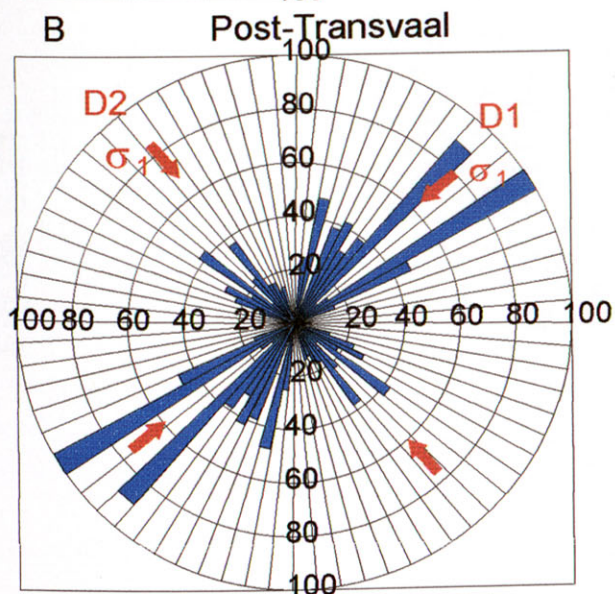
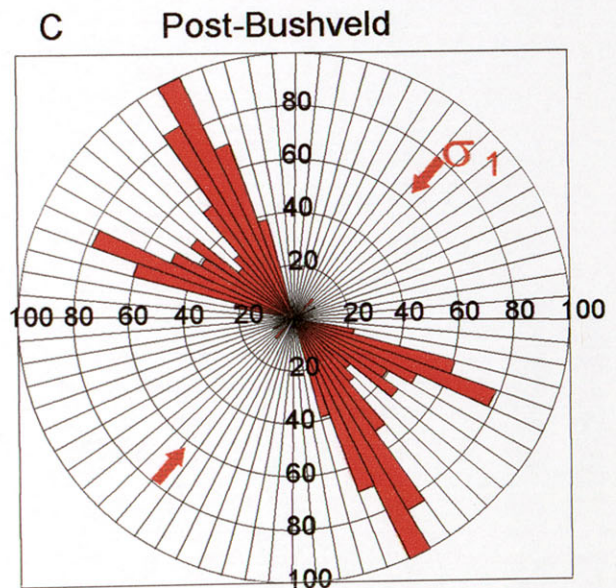
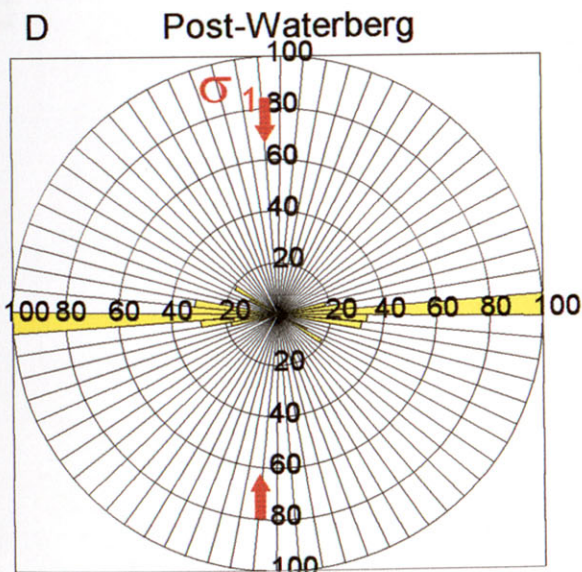
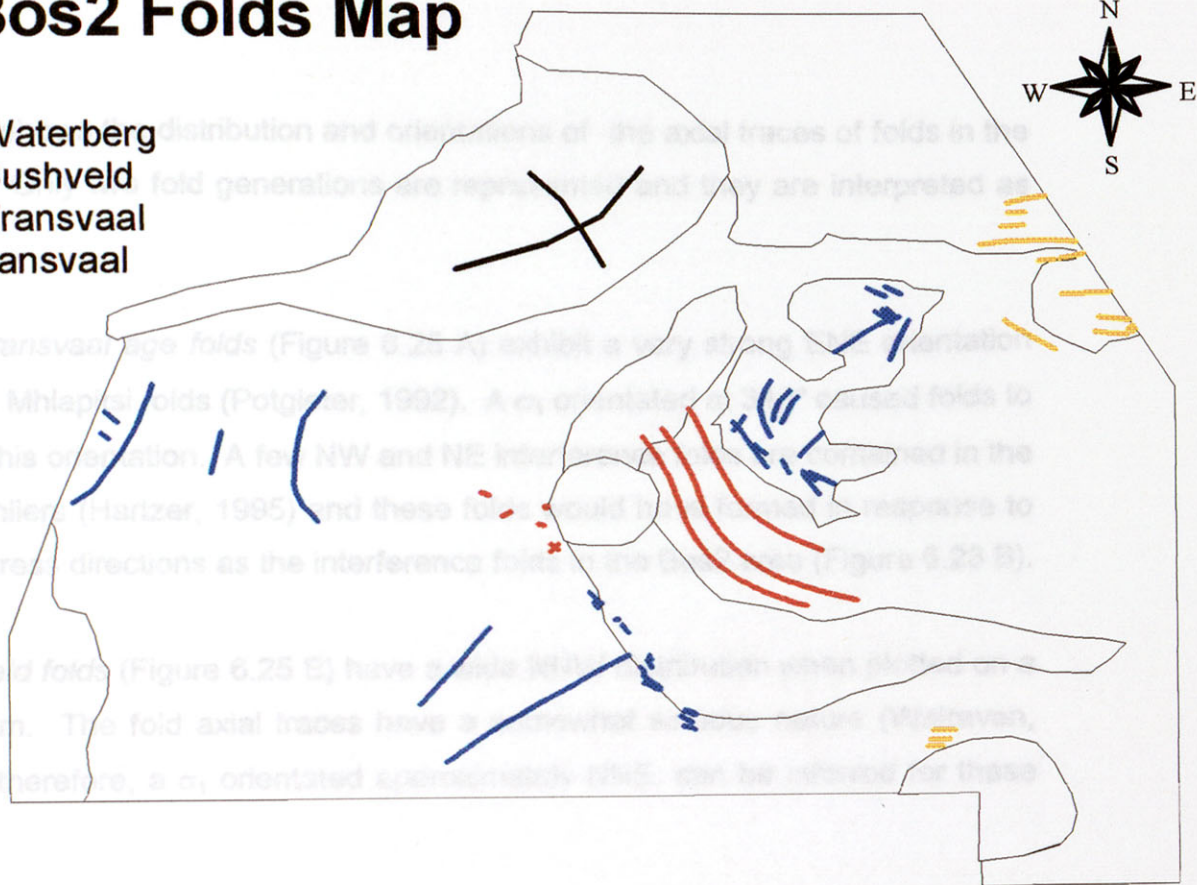


Figure 6.22 Bosgis Fold Map

Bos2 Folds Map

- D  Post-Waterberg
- C  Post-Bushveld
- B  Post-Transvaal
- A  Pre-Transvaal



6.4.3 Bos5

Figure 6.25 shows the distribution and orientations of the axial traces of folds in the Bos5 area. Only two fold generations are represented and they are interpreted as follows:

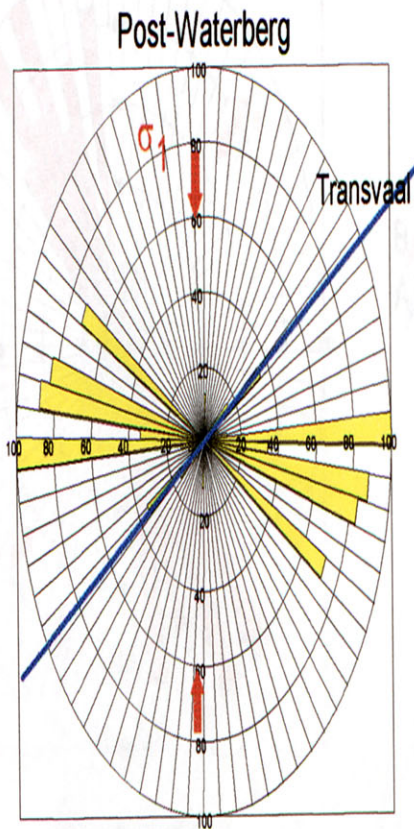
The *post-Transvaal age folds* (Figure 6.25 A) exhibit a very strong ENE orientation and reflects Mhlapitsi folds (Potgieter, 1992). A σ_1 orientated at 340° caused folds to develop in this orientation. A few NW and NE interference folds are contained in the Transvaal inliers (Hartzer, 1995) and these folds would have formed in response to the same stress directions as the interference folds in the Bos2 area (Figure 6.23 B).

The *Bushveld folds* (Figure 6.25 B) have a wide NNW distribution when plotted on a rose diagram. The fold axial traces have a somewhat sinuous nature (Walraven, 1986) and therefore, a σ_1 orientated approximately NNE, can be inferred for these folds.

Figure 6.24



Figure 6.24



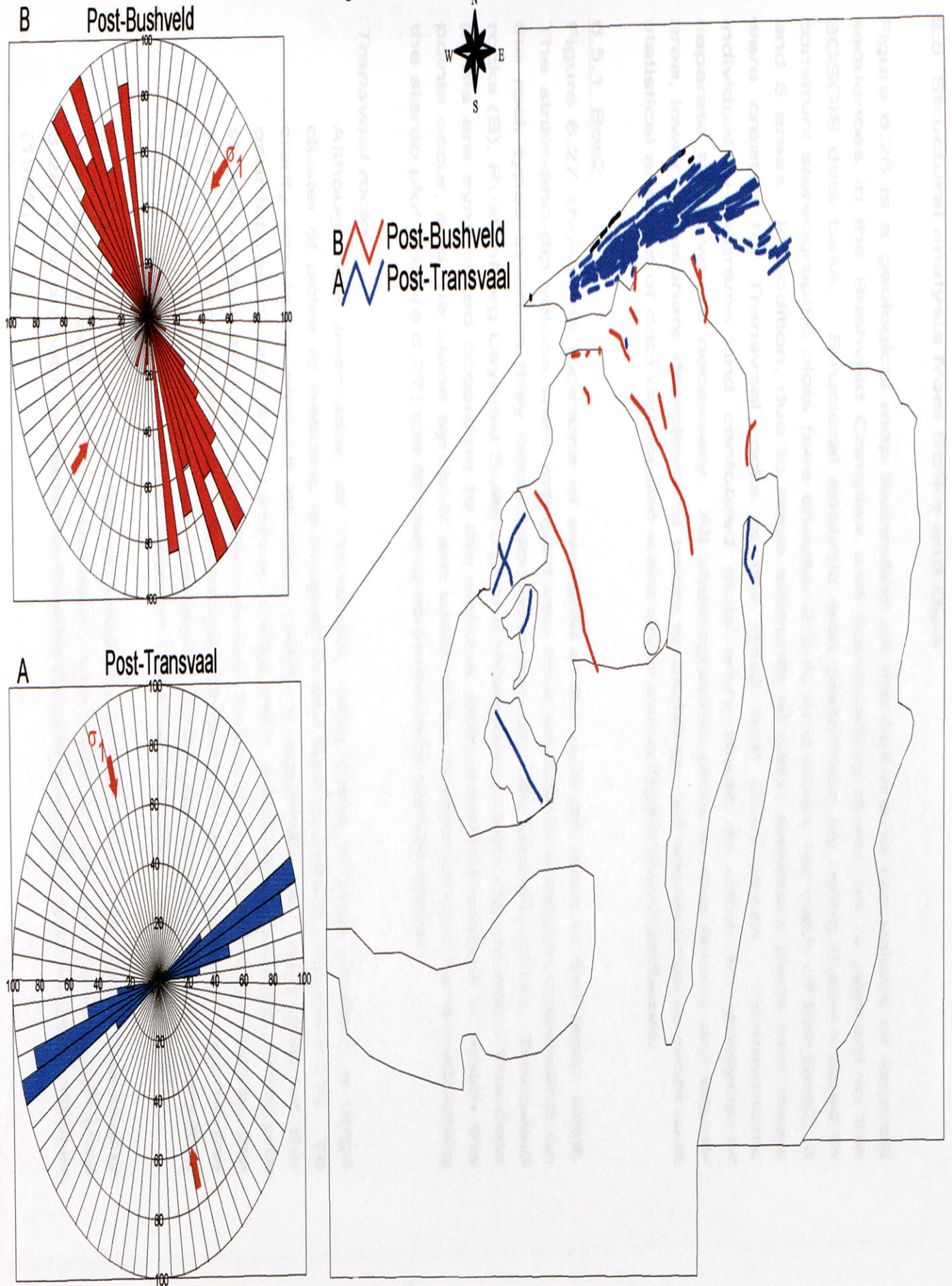
Bos3 fold Map



 Post-Waterberg
 Post-Transvaal

Figure 6.25

Bos5 fold Map



6.5 Structural analysis from Strike and Dips

Figure 6.26 is a geological map illustrating all the strike and dip values of layered sequences in the Bushveld Complex and surrounding areas as is present in the BOSGIS data base. Structural analysis was performed by using these values to construct stereographic plots (see chapter 2.3.4) and maps for each of the Bos2, 3 and 5 areas. In addition, due to large amounts of data, separate plots and maps were created for Transvaal rocks of the Bos2 and Bos5 areas. Furthermore, individual pi-diagrams and contoured plots were made to allow for analysis of separate areas where necessary. All stereographic plots in this thesis are equal-area, lower hemisphere depictions of poles to bedding. All stereographic plots and statistical analysis of data distribution were done using Spherical 2 software.

6.5.1 Bos2

Figure 6.27 shows the locations of available strike and dip data in the Bos2 area. The strike-and-dip values were grouped into four structural domains depending on the rock types in which they occur, domains include: an undefined (A), Transvaal rocks (B), Rustenburg Layered Suite (C) and Waterberg rocks (D) domain. The data points are symbolized according to the various stratigraphic horizons in which the points occur, and the same symbols are used in the stereonet plot from evaluating the stereo plot (Figure 6.27) the following observations can be made:

Transvaal rocks

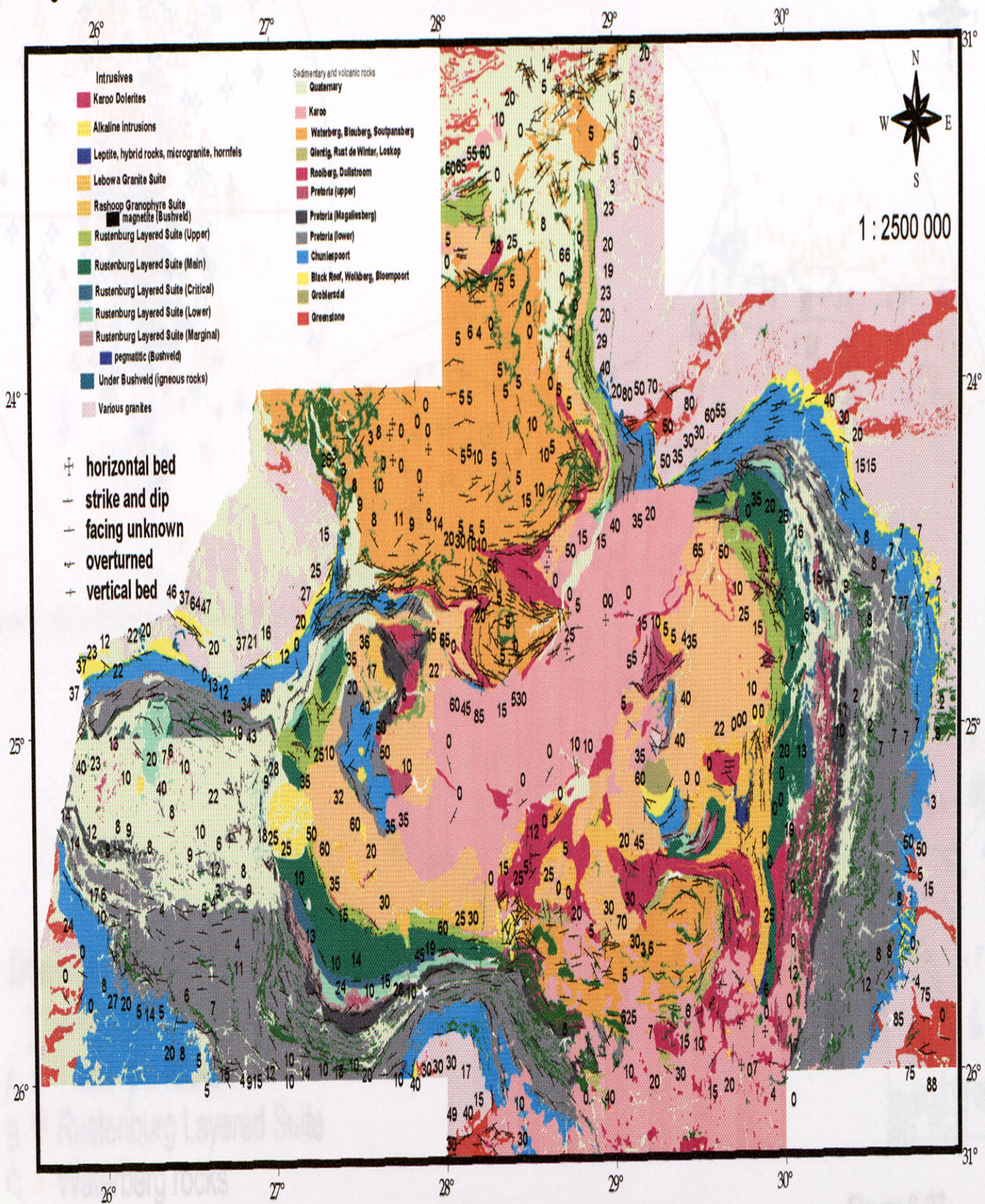
Although the orientation of Transvaal rocks have a wide scatter, a large cluster of poles to bedding is present in the SW quadrant (Figure 6.27). To clarify the large amount of data points a separate plot and map of the orientations of only the Transvaal rocks were made (Figure 6.28). This plot shows various structural domains of the Transvaal rocks as indicated by the similar colours on the map. Structural domains for the Bos2 area include the Transvaal inliers (A), western Transvaal basin (B), Johannesburg dome (C), Thabazimbi area (D) and far western Transvaal basin (E) (Figure 6.28).

It is evident that the bedding orientations in the Transvaal Inliers are highly variable as indicated by the scattered occurrence of poles to bedding (Figure 6.28). This probably reflects the interference fold pattern described by Hartzler (1995).

Map of the distribution of strike-and-dip values of Bos?

Figure 6.26

Bosgis Strike and Dip Map



Map of the distribution of strike-and-dip values of Bos2

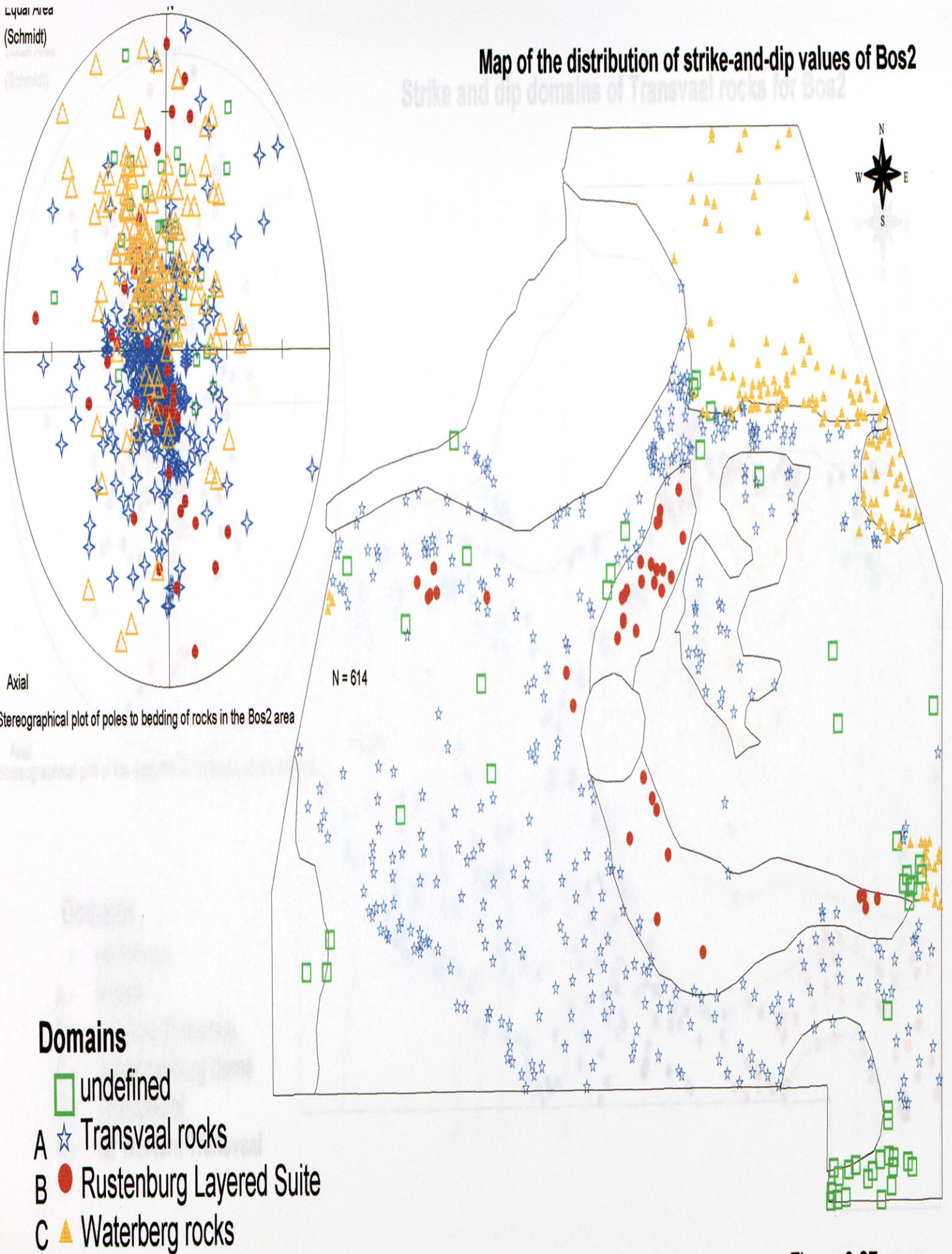
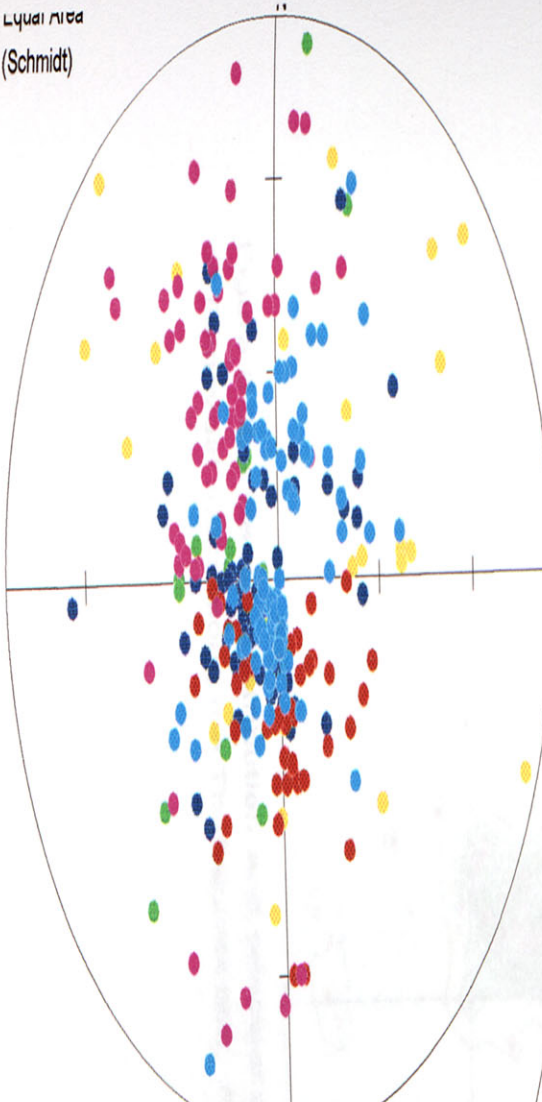
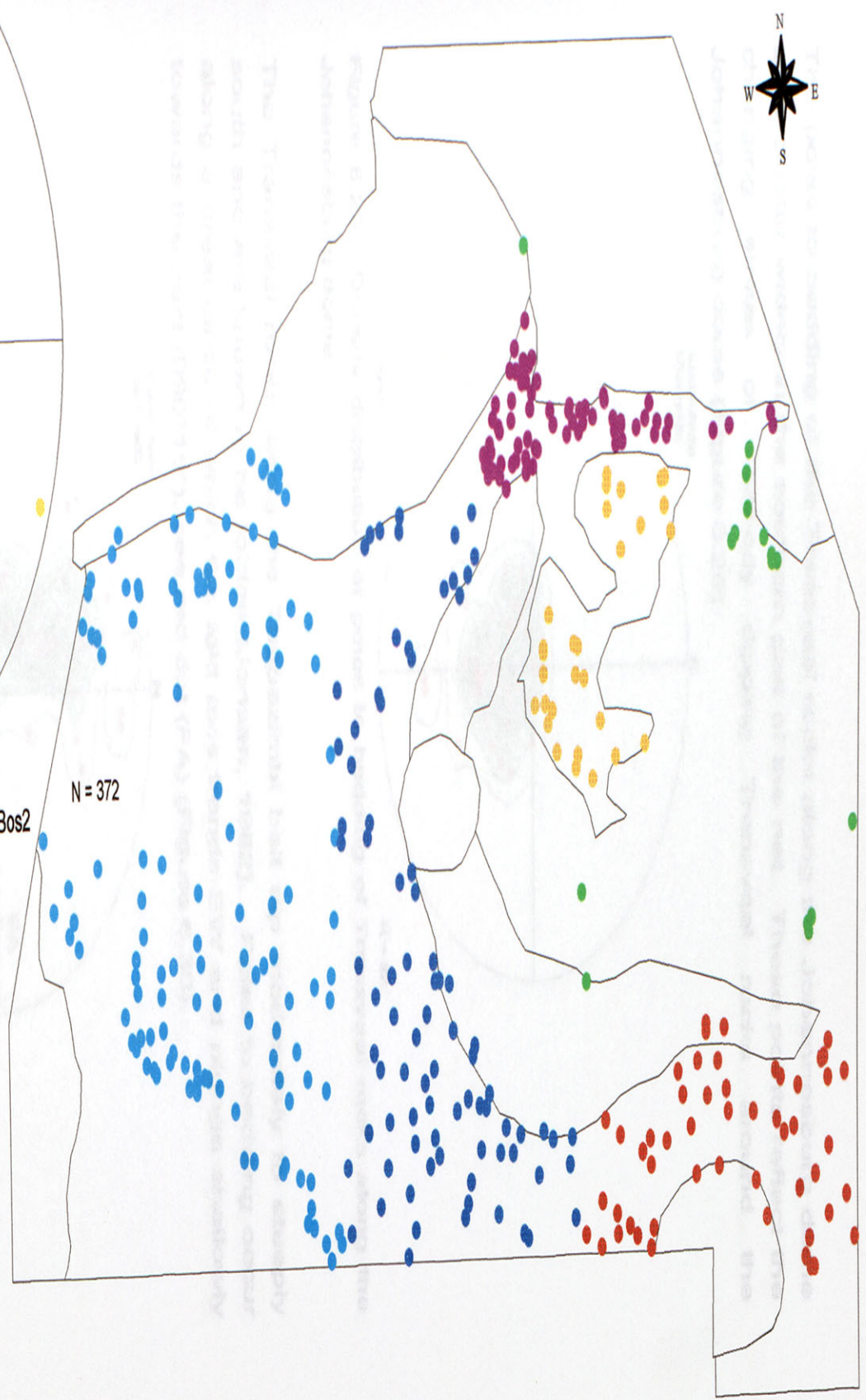


Figure 6.27

Strike and dip domains of Transvaal rocks for Bos2



Axial Stereographical plot of the domains of Transvaal rocks for Bos2



- Domains**
- undefined
 - A ● Inliers
 - B ● western Transvaal
 - C ● Johannesburg dome
 - D ● Thabazimbi
 - E ● far western Transvaal

Figure 6.28

The poles to bedding of the Transvaal rocks along the Johannesburg dome area cluster widely in the southern part of the net. These points reflect the changing strikes of northerly dipping Transvaal rocks around the Johannesburg dome (Figure 6.29).

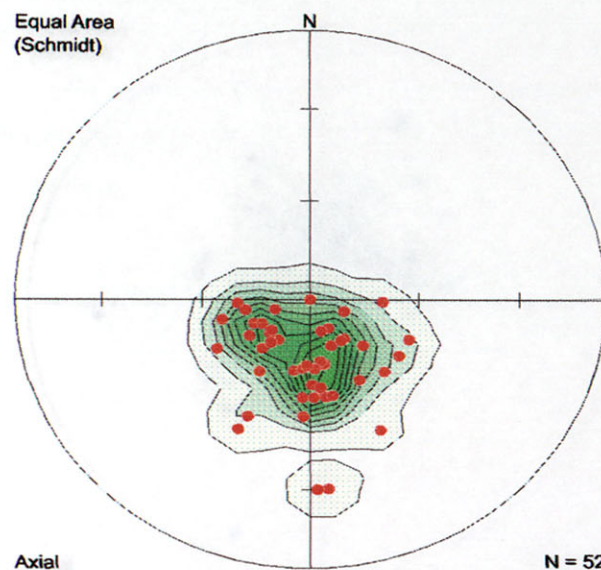


Figure 6.29. Density distribution of poles to bedding of Transvaal rocks along the Johannesburg dome.

The Transvaal rocks along the Thabazimbi belt dip moderately to steeply south and are known to be folded (Jansen, 1982). Poles to bedding occur along a great circle of which the fold axis trends EW and plunge shallowly towards the east ($090^{\circ}19'$), see red dot (FA) (Figure 6.30).

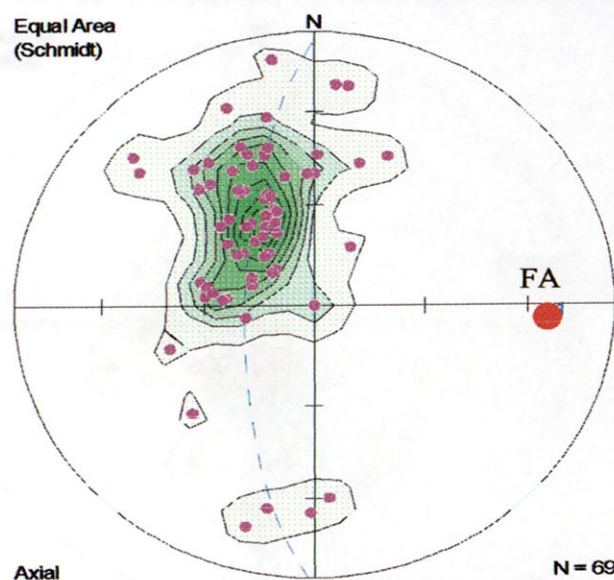


Figure 6.30. Density distribution and principal direction analysis of poles to bedding of Transvaal rocks along the Thabazimbi belt. FA = fold axis.

Poles to bedding of Transvaal rocks in the western and far western Transvaal basin (domains B + E) cluster in the center of the stereonet (Figure 6.31). This reflects Transvaal layers dipping of moderate angles towards the center of the main Transvaal basin.

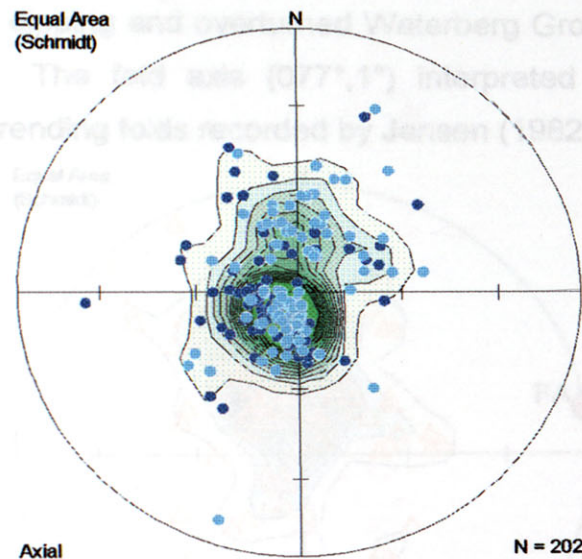


Figure 6.31. Density distribution analysis of poles to bedding of the western and far western Transvaal basin.

Bushveld Complex rocks

Poles to the layered sequences of the Bushveld Complex plot along a great circle as illustrated in Figure 6.32. A fold axis trending approximately EW and plunging shallowly E ($080^{\circ}, 8^{\circ}$) can be interpreted from the available data.

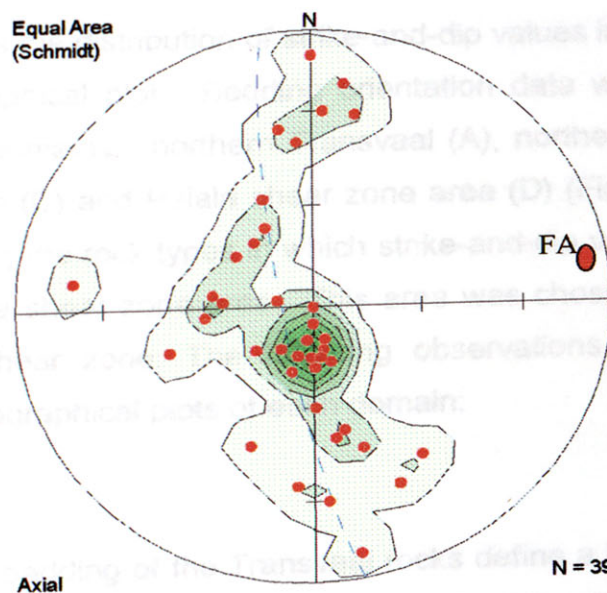


Figure 6.32. Density distribution and principal direction analysis of poles to layered sequences of the western lobe of the Bushveld Complex. FA = fold axis.

Waterberg Group rocks

Although the poles to bedding of Waterberg rocks cluster in the upper quadrants of the net, it also falls along a vague NS striking great circle (Figure 6.33). These poles generally signify EW striking and shallow southerly dipping to steeply dipping and overturned Waterberg Group rocks along the Thabazimbi belt. The fold axis ($077^{\circ}, 1^{\circ}$) interpreted from Figure 6.33 confirms the EW trending folds recorded by Jansen (1982).

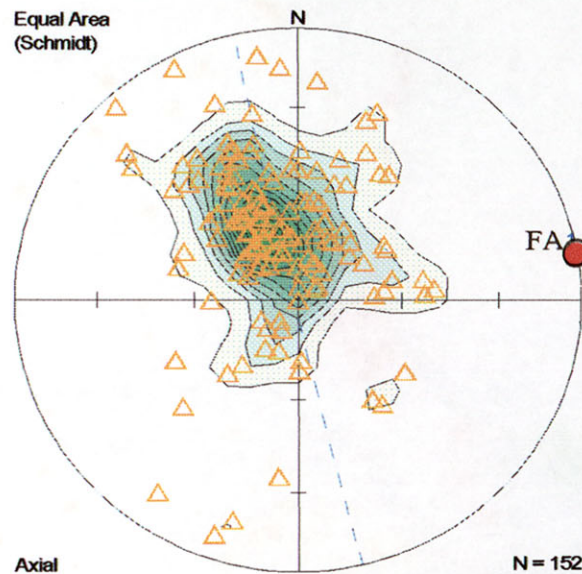


Figure 6.33. Density distribution and principal direction analysis of poles to bedding for Waterberg Group rocks of the Thabazimbi belt. FA = fold axis.

6.5.2 Bos3

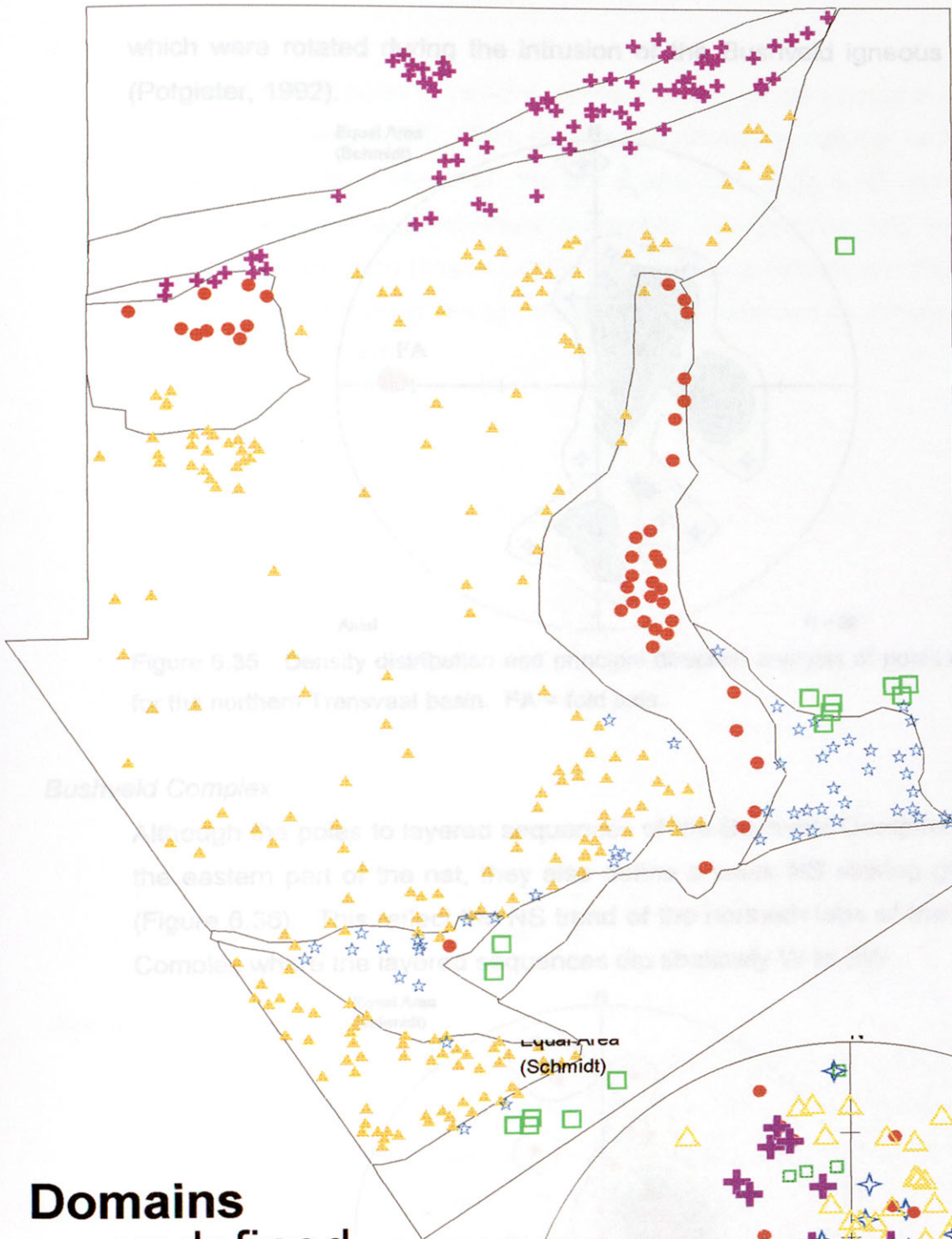
Figure 6.34 illustrates the distribution of strike-and-dip values in the Bos3 area with a composite stereographical plot. Bedding orientation data were grouped into the following structural domains; northern Transvaal (A), northern Bushveld Complex (B), Waterberg basin (C) and Palala shear zone area (D) (Figure 6.34). Domains are chosen according to the rock types in which strike-and-dip values were measured, except for the Palala shear zone area. This area was chosen based on outcrops along the Palala shear zone. The following observations can be made when evaluating the stereographical plots of each domain:

Transvaal rocks

The poles to bedding of the Transvaal rocks define a NS striking great circle (Figure 6.35). The fold axis (FA) calculated from the data distribution indicate a EW trending, shallow westerly plunging axis ($273^{\circ}19^{\circ}$). This reflects the folds in the Swaershoek area (Jansen, 1982) as well as Mhlapitsi-type folds

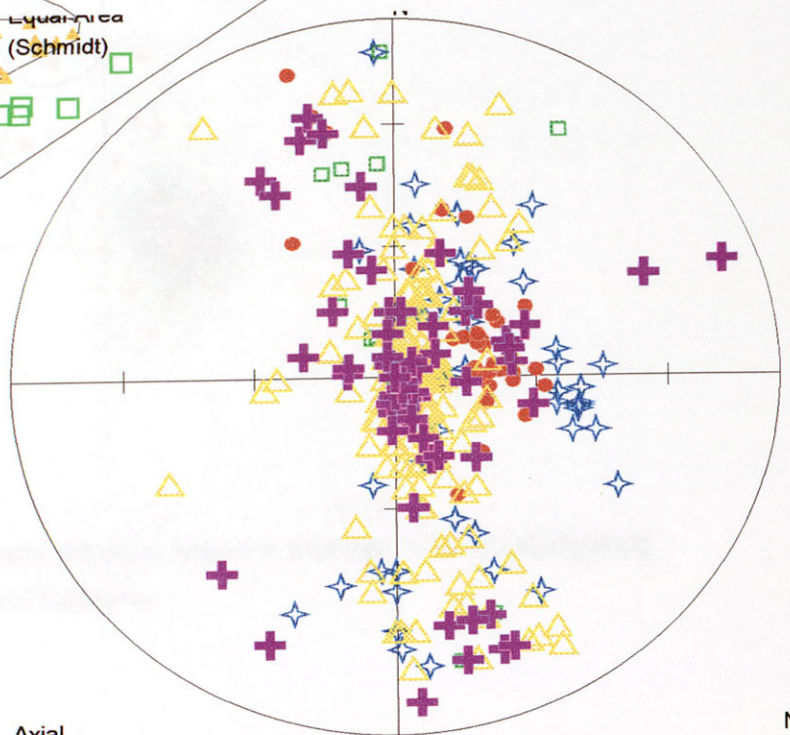
Figure 6.34

Map of strike and dip domains for Bos3



Domains

- undefined
- A ☆ Transvaal
- B ● Bushveld
- C ▲ Waterberg
- D + Palala



Axial

Stereographical plot of poles to bedding of domains of Bos3

N = 399

which were rotated during the intrusion of the Bushveld igneous Complex (Potgieter, 1992).

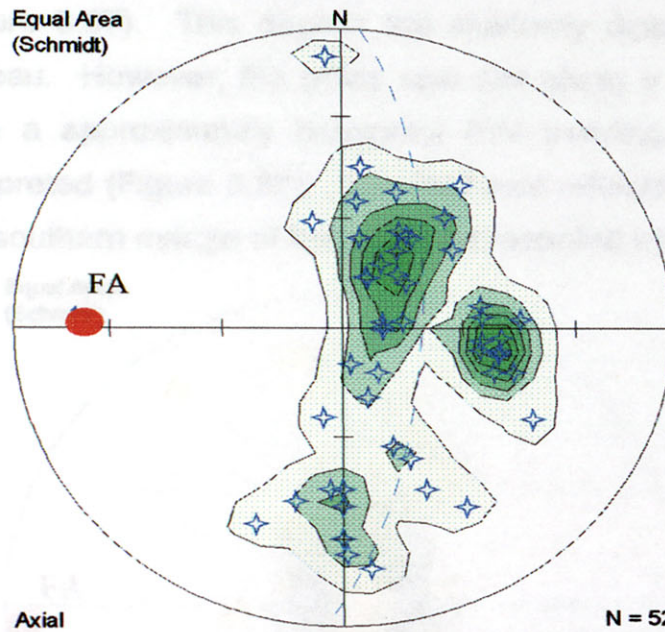


Figure 6.35. Density distribution and principal direction analysis of poles to bedding for the northern Transvaal basin. FA = fold axis.

Bushveld Complex

Although the poles to layered sequences of the Bushveld Complex cluster in the eastern part of the net, they also define a weak NS striking great circle (Figure 6.36). This reflects the NS trend of the northern lobe of the Bushveld Complex where the layered sequences dip shallowly W to SW.

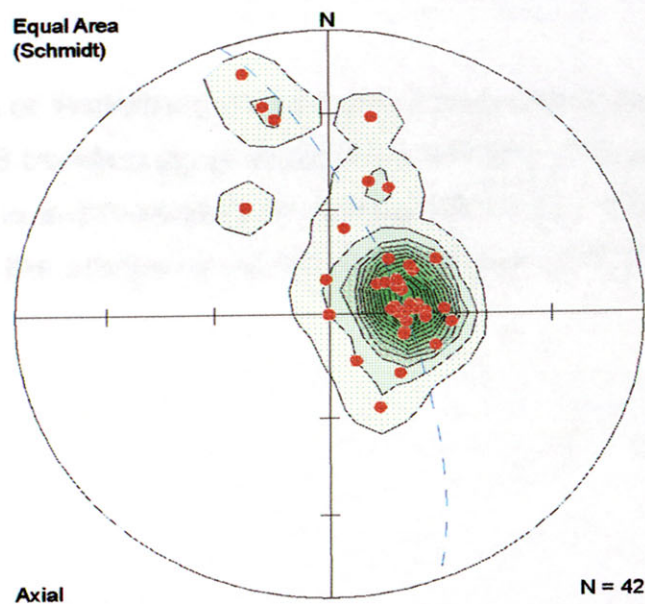


Figure 6.36. Density distribution and principal direction analysis of poles to layering for the northern lobe of the Bushveld Complex.

Waterberg Group

A large cluster of poles to bedding of the Waterberg rocks occur in the center of the net (Figure 6.37). This depicts the shallowly dipping rocks on the Waterberg plateau. However, the poles also plot along a NS striking great circle for which a approximately horizontal EW trending fold axis (FA = $266^{\circ}, 4^{\circ}$) is interpreted (Figure 6.37). This fold axis reflects the EW trending folds along the southern margin of the basin as recorded by Jansen (1982).

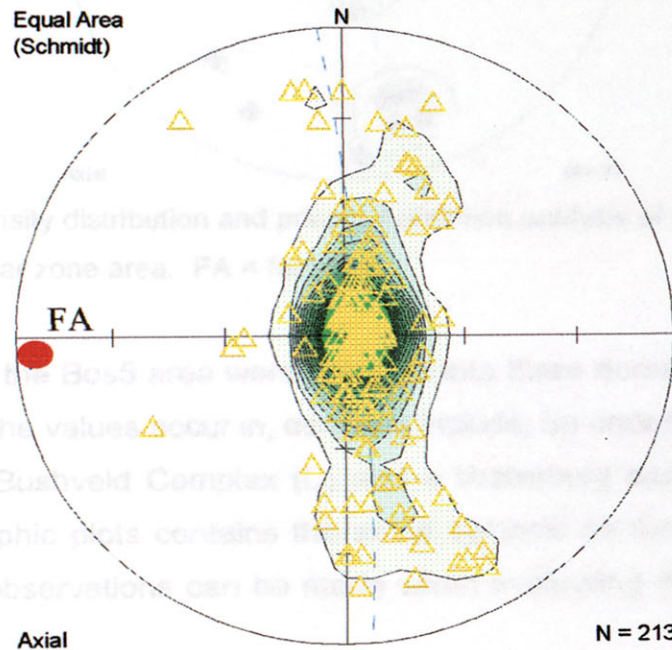


Figure 6.37. Density distribution and principal direction analysis of poles to bedding for the Waterberg plateau. FA = fold axis.

Palala shear zone area

Poles to bedding of Waterberg rocks in the Palala shear zone area define an approximately NS trending great circle (Figure 6.38). The calculated fold axis trends ENE and is approximately horizontal ($261^{\circ}, 3^{\circ}$). The trend of the fold axis is parallel to the orientation of the Palala shear zone (Figure 4.5).

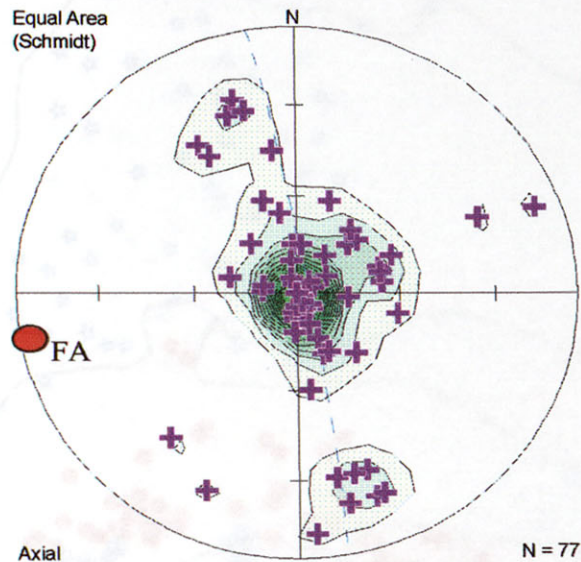


Figure 6.38. Density distribution and principal direction analysis of poles to bedding in the Palala shear zone area. FA = fold axis.

6.5.3 Bos5

Strike and dip data of the Bos5 area were grouped into three domains according to the ages of the rocks the values occur in, domains include; an undefined domain (A), Transvaal rocks (B), Bushveld Complex (C) and a Waterberg domain (D) (Figure 6.39). The stereographic plots contains the same symbols as the domains of the map. The following observations can be made when evaluating the stereographic plots.

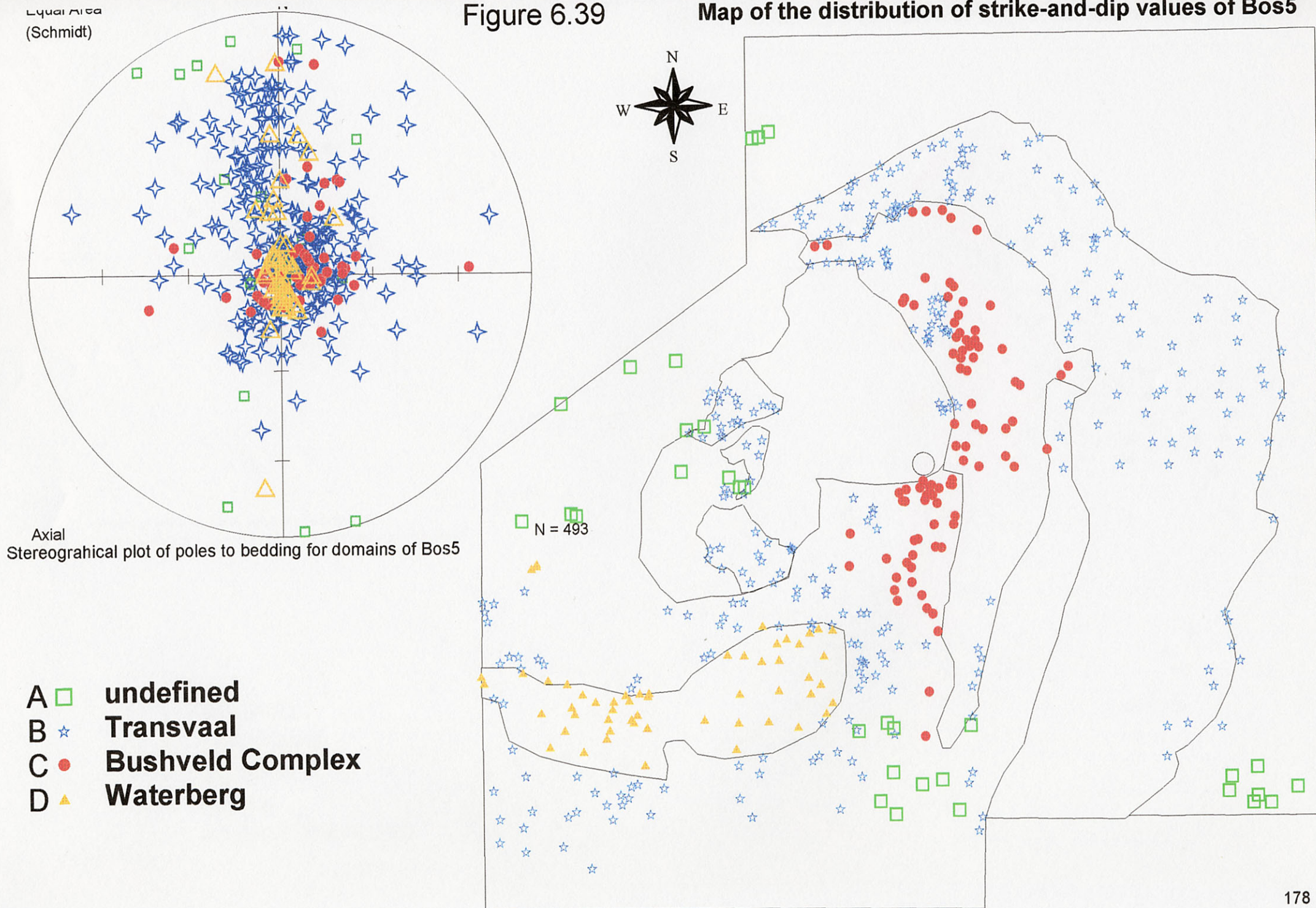
Transvaal rocks

Structural domains for the Transvaal rocks were further subdivided and include the Mhlapitsi fold belt (A), Transvaal inliers (B) and eastern Transvaal basin (C) (Figure 6.40). Similar to Transvaal inliers in the Bos2 area, the poles to bedding of the inliers occurring in the eastern Bushveld Complex are scattered throughout the stereonet (Figure 6.40). The scatter probably reflects the interference fold pattern of the inliers as documented by Hartzler (1995).

The poles to bedding of Transvaal rocks along the Mhlapitsi fold belt cluster in the NNW area of the stereonet, but also lie along a weak NNW great circle (Figure 6.41). A horizontal ENE trending fold axis (FA = $075^{\circ}/0^{\circ}$) calculated from this data. Mhlapitsi-type folds recorded by Potgieter (1992) differs from the fold axis of Figure 6.41, in that Mhlapitsi-folds trend more NE and plunges steeply west. This variance might be due to the lack of data in the BOSGIS database.

Figure 6.39

Map of the distribution of strike-and-dip values of Bos5



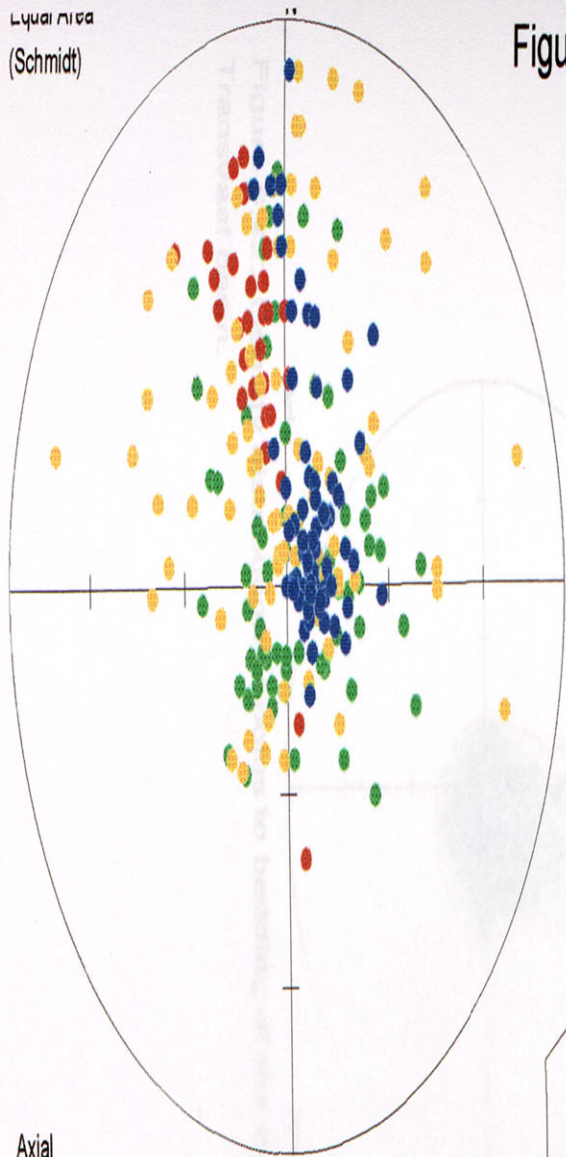
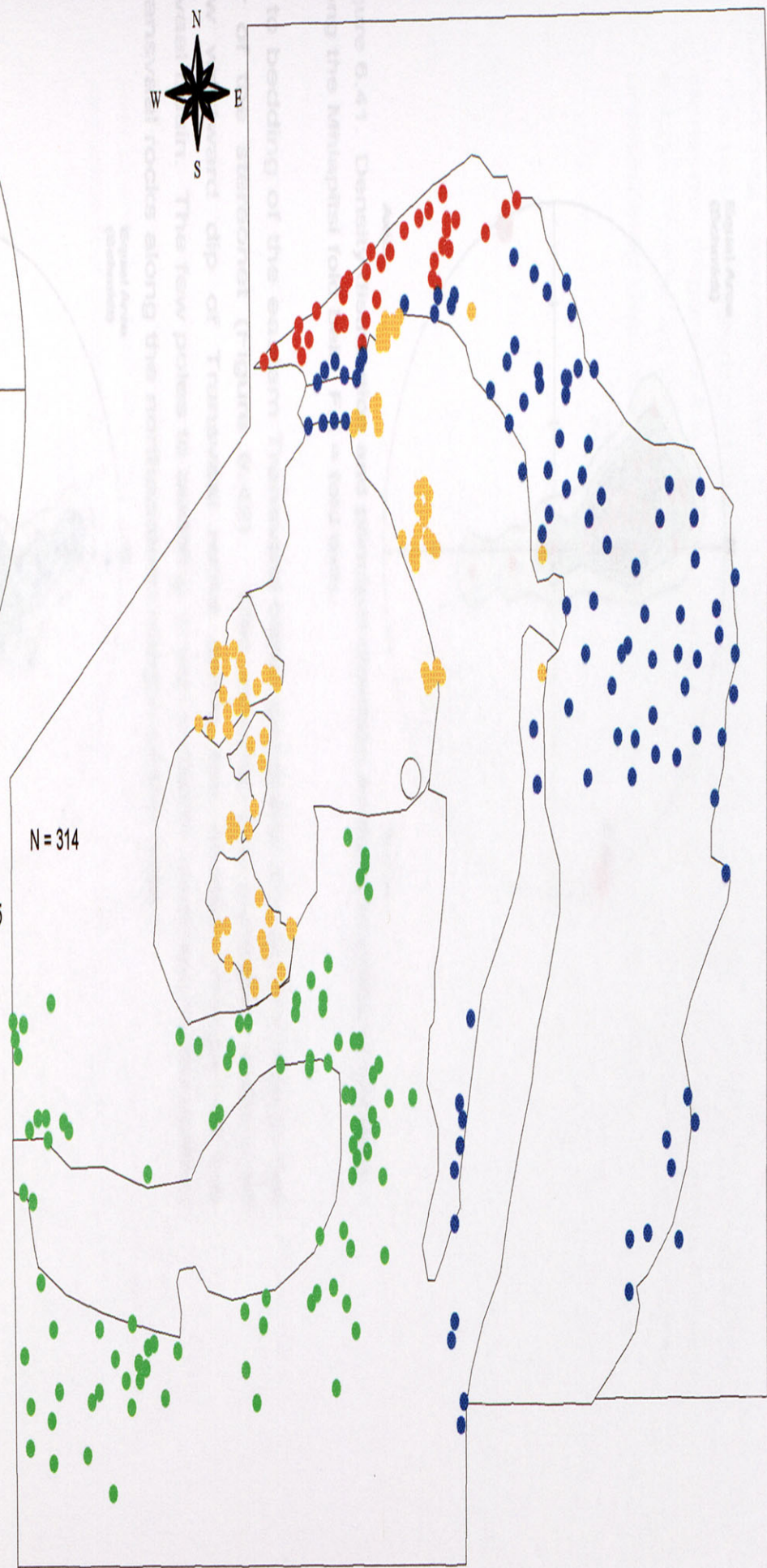


Figure 6.40

Map of strike and dip domains of Transvaal rocks for Bos5



Stereographical plot of poles to bedding of Transvaal rocks illustrating the various domains for Bos5

- Domains**
- undefined
 - A ● Mlapitsi
 - B ● Inliers
 - C ● eastern Transvaal

Rustenburg Layered Suite

The pole clustering of the Rustenburg Layered Suite (Rustenburg) is the center of the stereonet (Figure 6.43). The poles to bedding of the Rustenburg rocks (Figure 6.42). This is an undeformed nature of the

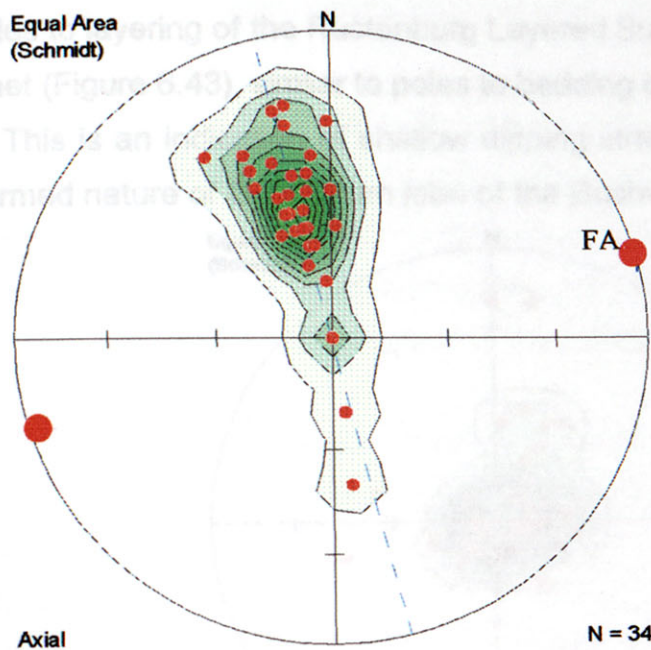


Figure 6.41. Density distribution and principal direction analysis of poles to bedding along the Mhlapitsi fold belt. FA = fold axis.

Poles to bedding of the eastern Transvaal basin generally cluster strongly in the center of the stereonet (Figure 6.42). This reflects the constant strike and shallow westward dip of Transvaal rocks along the eastern margin of the Transvaal basin. The few poles to bedding which indicate southward dips reflect the Transvaal rocks along the northeastern margin of the basin.

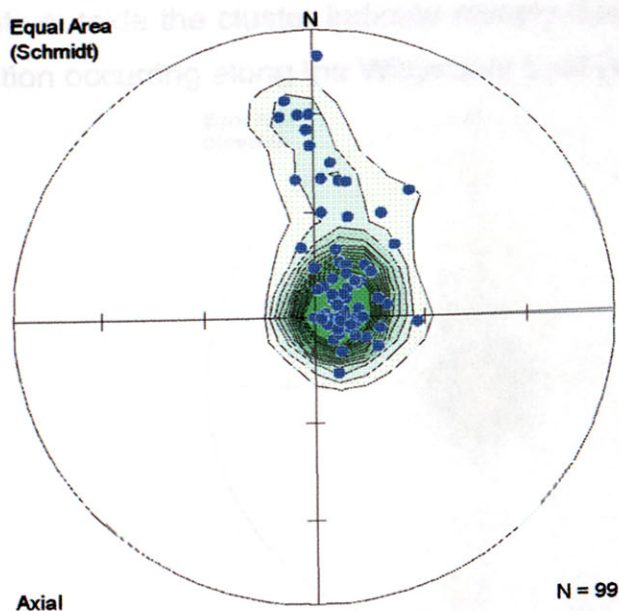


Figure 6.42. Density distribution of poles to bedding of the eastern margin of the Transvaal basin.

Rustenburg Layered Suite

The poles to layering of the Rustenburg Layered Suite cluster in the center of the stereonet (Figure 6.43), similar to poles to bedding of the Transvaal rocks (Figure 6.42). This is an indication of shallow dipping strata, and reflects the generally undeformed nature of the eastern lobe of the Bushveld Complex.

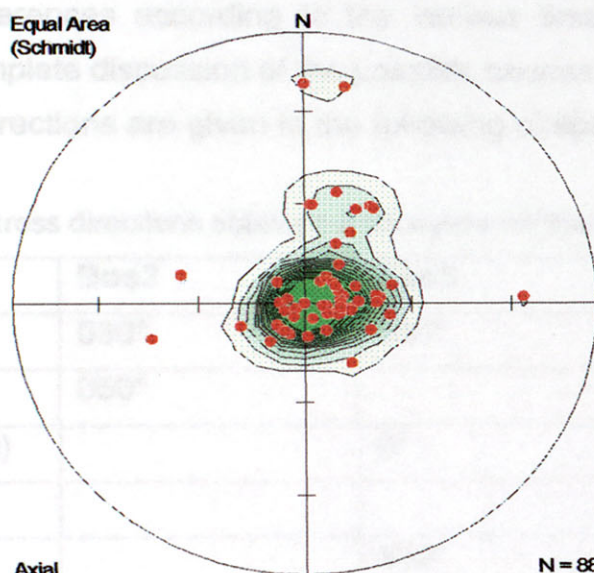


Figure 6.43. Density distribution of poles to layering of the eastern lobe of the Bushveld Complex.

Waterberg rocks

The poles to bedding of Waterberg rocks cluster more or less in the center of the net (Figure 6.44) signifying the shallow dips of the Cullinan-Waterberg basin. A few points outside the cluster indicate steeply dipping strata associated with the deformation occurring along the Wilgerivier fault (Van der Neut, 2000).

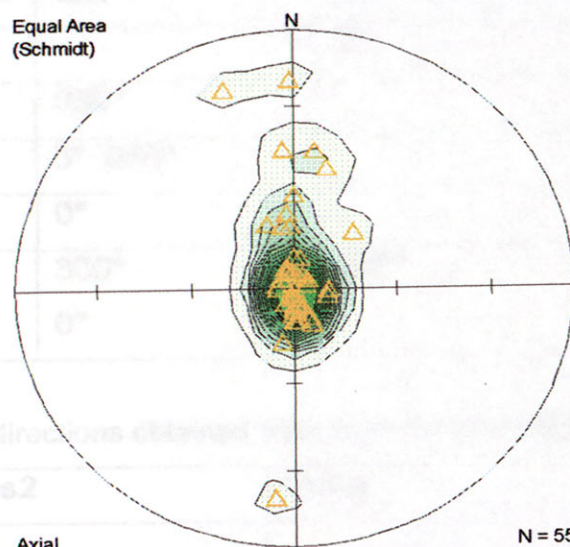


Figure 6.44. Density distribution of poles to bedding of Cullinan-Waterberg basin.

6.6 Summary of stress orientations derived from all the structural features

Stress directions obtained from the various structures, in the different regions and of the same age are summarized in Tables 6.1 – 6.4. These directions are compared for similarities and differences according to the various time periods considered during this study. A complete discussion of the possible causes and regional tectonic histories of the stress directions are given in the following chapter.

Table 6.1 Summary of σ_3 stress directions obtained from dykes for the respective Bos areas.

Domains	Bos2	Bos3	Bos5
Dolerite (post-Karoo)	030°	030°	030°
Syenite (Pilanesberg)	050°		
Makgabeng (Waterberg)		0°	
Transvaal rocks			310°
Archaean rocks		330°	320°

Table 6.2 Summary of σ_3 directions obtained from lineaments for the respective Bos areas.

Domains	Bos2	Bos3	Bos5
Undefined	0°		
Pilanesberg	radial		
Waterberg	020°	0°	
Palala		0°	
Rooiberg	030°		
Western Transvaal	0° 060°		
Far western Transvaal	0°		290°
Archaean	330° 0°	350°	350°

Table 6.3 Summary of σ_1 directions obtained from folds for the respective Bos areas.

Age	Bos2	Bos3	Bos5
Post-Waterberg	NS	NS	
Post-Bushveld	NE		NE
Post-Transvaal	NW and NE		340° NW
Pre-Transvaal	NW and NE		

Table 6.4

Summary of stress orientations of the respective Bos areas obtained from faults.

Age	Bos2						Bos3						Bos5					
	Age1			Age2			Age1			Age2			Age1			Age2		
	σ_1	σ_2	σ_3	σ_1	σ_2	σ_3	σ_1	σ_2	σ_3	σ_1	σ_2	σ_3	σ_1	σ_2	σ_3	σ_1	σ_2	σ_3
Post-Karoo	v	60°	330°				v	70°	340°				v	90°	0°			
Post-Pilanesberg	v	h	h															
Post-Waterberg	0°	90°	v							50°	v	320°	0°	90°	v			
	v	290°	40°							0°	080°	v						
Post-Bushveld	v	330°	60°							30°	v	300°				v	50°	320°
Post-Transvaal	340°	v	70°	v	340°	60°	30°	v	300°				0°	v	270°	v	60°	330°
	v	h	h															
Syn-Transvaal	v	330°	60°							330°	60°	v				330°	60°	v
Pre-Transvaal	30°	v	300°				30°	v	300°	90°	v	0°	30°	v	300°			

Pre-Transvaal

Although, structural line data for the pre-Transvaal period is scarce, the stress directions indicated by analyses of available dykes, lineaments and faults in all the Bos areas display fairly similar σ_3 directions of between 300° and 350° . A secondary, σ_3 direction of 0° obtained for Bos2 lineaments and Bos3 Age2 faults are also evident.

Syn-Transvaal

Syn-Transvaal σ_1 directions of 330° from faults for the Bos3 and Bos5 areas correspond with each other, but not the stress directions of the faults of the Bos2 area. However, the stress directions of the Bos2 area matches post-Transvaal directions derived from the Bos2 Age2 faults. It is however interesting to note that more or less the same stress directions are constantly repeated by σ_1 , σ_2 and σ_3 stresses during syn-Transvaal and post-Transvaal times. These directions are $330/340^\circ$ and $60/70^\circ$.

Post-Transvaal

Most of the dykes and lineaments occurring in Transvaal rocks indicate σ_3 directions varying between 290° and 0° . Stress directions interpreted from faults during this time period also rendered σ_3 directions varying between 270° and 330° . However, a second σ_3 direction varying between 060° and 070° is also evident from post-Transvaal faults and lineaments. In addition σ_1 directions trending NW and NE corresponds to σ_1 directions of 340° and 30° of Bos2 and Bos3 areas respectively.

Post-Bushveld

Stress directions obtained from the faults varying between 030° to 060° and are constantly repeated by σ_1 , σ_2 and σ_3 directions. However, NE trending σ_1 directions obtained from fold analysis of the Bos2 and Bos5 areas are at variance with stresses obtained from the fault analysis.

Post-Waterberg

Dykes and lineaments occurring in the Waterberg domains exhibit σ_3 directions of 0° , whereas stress analyses from faults and folds indicates σ_1 trending generally 0° . However, some stress directions from Waterberg faults in the Bos3 area do not correspond to any of the above mentioned directions.

7. DISCUSSION

Pilanesberg

Stress directions interpreted for the Pilanesberg age were only obtained from the Bos3 area. The syenite dykes indicates a σ_3 direction of 050° and a vertical σ_1 , whereas stress directions for the faults and lineaments around the dome indicate a radial horizontal σ_3 pattern, and also a vertical σ_1 .

Post-Karoo

Post-Karoo dolerite dykes in each of the Bos areas rendered a σ_3 direction of 030°. However, stress directions obtained from fault analyses do not confirm this direction, and indicates a σ_3 directions between 330° to 0°.

explanations for the causes of these stress directions, due to the lack of detailed structural information about these structures, although some stress ellipses are considered and altered, as respectively, the structural development style of such structures are discussed.

The time periods which are considered include, the pre-Transvaal, post-Transvaal/pre-Bushveld, post-Bushveld/pre-Pilanesberg, Pilanesberg and post-Karoo periods. In this study, the regional tectonic events, local events, the development of the Transvaal and the present the possible stress ellipses for each of these periods.

7.1 Pre-Transvaal

The pre-Transvaal time bracket includes the period from the formation of the Kaapvaal Craton was subjected to a major tectonic event, the formation of the craton. During this time variously orientated compressional structures, including radial and subsequent basin formation. The evolution prominent stress directions throughout the later history of the craton, including the formation of greenstone belts as well as important lineaments, such as the Barberton and Barbarton lineament. Pre-Transvaal structures, such as the Barbarton lineament, as well as NNW orientated structures. The evolution of the pre-Transvaal structures in the Bushveld region, including the formation of the Bushveld Complex during this time are not well represented.